PACKING, SINTERING AND BLENDING OF BINARY POWDER MIXTURES

By

GARY LYNN MESSING

A DISSERTATION PRESENTED TO THE GRADUATE COUNCIL OF
THE UNIVERSITY OF FLORIDA
IN PARTIAL FULFILLMENT OF THE REQUIREMENTS FOR THE
DEGREE OF DOCTOR OF PHILOSOPHY

UNIVERSITY OF FLORIDA

1977

To Becky and Dad

ACKNOWLEDGEMENTS

The author wishes to express his gratitude to each of the members of his committee, G. Y. Onoda, Jr., F. N. Rhines, R. T. DeHoff, L. L. Hench and R. Schaeffer, who each helped in his own way. He would especially like to thank G. Y. Onoda, Jr., for his perseverance and patience throughout the course of this work as well as for a research philosophy. Many thanks to F. N. Rhines for a fundamental perspective.

In addition, thanks are extended to J. M. Horn, Jr., J. Adair and B. Patterson for helpful discussions. The technical assistance of M. Stoufer is gratefully acknowledged.

The author acknowledges the Pratt and Whitney Aircraft Corporation for partial financial support.

Finally, many thanks to Becky, my wife.

TABLE OF CONTENTS

		Page
ACKNOWLEDGEMENTS		iii
LIST OF FIGURES		iv
LIST OF TABLES		vii
ABSTRACT		viii
CHAPTER		
I	INTRODUCTION	1
	Overview	1
	Research Plan	5
II	INHOMOGENEITY-PACKING DENSITY RELATIONS IN BINARY POWDERS	7
	Introduction	7
	The Furnas Theory	9
	Local Compositional Variations and Specific Volume	13
	The Degree of Mixedness Parameter	19
	Hypothetical Examples	23
	Discussion and Summary	30
III	INHOMOGENEITY-PACKING DENSITY RELATIONS IN BINARY POWDERS--EXPERIMENTAL STUDIES	33
	Introduction	33
	One-Dimensional Packing	34
	Three-Dimensional Packings	43
	Summary	50

Page

IV THE SINTERING OF INHOMOGENEOUS BINARY POWDER MIXTURES..... 52

Introduction..... 52
Theory..... 53
Fines Sintering Only..... 54
Coarse and Fines Sintering..... 59
Discussion of Results..... 68
Summary..... 72

V VIBRATORY BLENDING OF METAL POWDERS..... 73

Introduction..... 73
The Nature of Vibratory Blending..... 75
Principles..... 75
Observations..... 79
Experimental Procedure..... 82
Experimental Results..... 89
Discussion and Summary..... 101

VI CONCLUSIONS..... 106

APPENDIX..... 109

BIBLIOGRAPHY..... 115

BIOGRAPHICAL SKETCH..... 117

LIST OF FIGURES

Figure		Page
1	Theoretical binary packing relations of Furnas.	11
2	Schematic integration areas for calculating $(\tilde{w}_f)_I$ and $(\tilde{w}_f)_{II}$ from w_f-Q data.	20
3	Theoretical compositional variations with increased mixing in a horizontal mixer.	25
4	The calculated specific volume, $\hat{v}$, normalized by the theoretical volume, v_o, of the particles, at various levels of mixing, assuming the Lacey distribution.	27
5	The calculated specific volume, $\hat{v}$, normalized by the theoretical volume, v_o, of the particles, at various levels of mixing, assuming the normal distribution.	29
6	Comparison of the hypothetical data and two proposed relationships for the effect of mixing on the bulk density at $\tilde{w}_f = 0.3$.	31
7	Sampling container for analysis of one-dimensional compositional variation.	35
8	Compositional distribution curve for $\tilde{w}_f = 0.254$ with M = 0.275 for one-dimensional compositional variation.	38
9	Experimental w_f versus cumulative weight fraction from the top of the stack curves for $\tilde{w}_f = 0.323$ and for one-dimensional compositional variation.	39
10	Experimental w_f versus cumulative weight fraction from the top of the stack curves for $\tilde{w}_f = 0.254$ and for one-dimensional compositional variation.	40

Figure		Page
11	The Furnas, the experimental and local Furnas specific volumes versus the mixedness parameter for $\overset{\vee}{w}_f$ equal to 0.323 and 0.254.	42
12	Sampling container and thief sampler for analyzing three-dimensional compositional variation.	44
13	Experimental compositional variation curves for $\overset{\vee}{w}_f$ = 0.254.	46
14	Experimental compositional variation curves for $\overset{\vee}{w}_f$ = 0.150 and 0.325.	47
15	The relative shrinkage of binary mixtures at various levels of sintering for two levels of homogeneity when only the fines sinter.	58
16	The relative shrinkage during sintering for two average compositions and two levels of homogeneity when only the fines sinter.	60
17	Hypothetical sintered volumes for compositions between w_f^* and w_{fs}^m, assuming a linear relation.	62
18	The relative shrinkage for fines sintering faster than the coarse particles for three stages of sintering and two levels of homogeneity.	64
19	The relative shrinkage as a function of the change in the specific volumes of the fines and coarse particles for three stages of sintering and two levels of homogeneity.	67
20	Experimental data of O'Hara and Cutler [5] for the relative linear shrinkage for different compositions after two constant sintering times (minutes).	69
21	The flow pattern of a particle bed at a frequency of 2100 rpm, demonstrating the three main blending regimes.	80
22	Blending container.	83

Figure		Page
23	Photograph of blending apparatus showing a) blending container, b) container holder, c) motor, d) unbalanced wheel, and e) softspring.	87
24	The change in the compositional distribution in the stack with progressive blending at 1800 rpm.	90
25	Time variation for blending at five different frequencies for a mixture having a radius ratio of 1.0.	92
26	The rate of blending of a binary powder in three differently sized containers.	94
27	The degree of mixedness after thirty minutes of blending for various size ratios.	96
28	The rate of blending for binary mixtures with a size ratio of 1.7 at two different compositions (w_f = 0.1 and 0.9).	98
29	The influence of size distribution on the rate of blending for a binary mixture having a radius ratio of 1.0.	100
30	The influence of size distribution on the rate of blending for a binary mixture having a radius ratio of 1.7 (w_f = 0.1 and 0.9).	102
31	The influence of size distribution on the rate of blending for a binary mixture having a radius ratio of 1.7 (w_f = 0.5).	103

LIST OF TABLES

Table		Page
I	Experimental and theoretical specific volumes for three-dimensional compositional variations for $\hat{w}_f$ equal to 0.325 and 0.150.	48
II	Experimental and theoretical specific volumes for three-dimensional compositional variations for $\hat{w}_f$ equal to 0.254 (w_f^*).	49
III	Physical characteristics of powders.	85
IV	Sieve mixtures for different radius ratios.	86

Abstract of Dissertation Presented to the Graduate Council of the University of Florida in Partial Fulfillment of the Requirements for the Degree of Doctor of Philosophy

PACKING, SINTERING AND BLENDING OF BINARY POWDER MIXTURES

by

Gary L. Messing

December, 1977

Chairman: George Y. Onoda, Jr.
Major Department: Materials Science and Engineering

In various phases of powder processing compositional inhomogeneities give rise to deviations from ideal behavior. Commonly, these deviations are attributed, without theoretical justification, to either powder or process variables. In the case of binary powder mixtures with large size differences this has been because of the absence of a fundamental means to test the original theory. In this work mathematical procedures are presented to permit the assessment of the contribution of compositional inhomogeneities for particle packing and sintering. Also, a fundamental evaluation of vibratory blending is given from which meaningful methods of reducing inhomogeneities can be developed.

For the packing of binary powder mixtures a theoretical methodology has been developed which makes possible the calculation of the specific volume of an inhomogeneous mixture. The procedure is based on the hypothesis that the Furnas model is valid on a local level. Using two hypothetical examples it is demonstrated that the specific volume-composition curves calculated by the methodology have shapes resembling typical experimental data.

To test the hypothesis, inhomogeneous binary powder mixtures of glass microbeads were sampled and the compositional inhomogeneity data used to calculate the specific volume. It was demonstrated that calculated specific volumes correspond to the bulk specific volumes of the samples, thus proving the hypothesis.

The methodology was applied to the sintering of inhomogeneous binary powder mixtures and a procedure developed to calculate the shrinkage during sintering. With a hypothetical example deviations from ideal shrinkage curves due to inhomogeneities were demonstrated. Furthermore, these results were shown to be similar to experimental data in the literature. The usefulness of the methodologies for packing and sintering is that the effects of additional variables to the packing or sintered volumes can be recognized, because contributions to the volume due to inhomogeneities can be determined and eliminated.

Despite the prevalence of blending procedures to eliminate inhomogeneities, little is understood about the fundamental nature of these processes. By assessing the interparticle behavior for vibratory blending it is shown that the ultimate level of homogeneity depends on the connectivity of the particle mass and the energetics of the system. Also, it is demonstrated that blending in this system is dependent on the interaction of the convective and diffusive mechanisms.

CHAPTER I
INTRODUCTION

Overview

In the past fifty years a considerable amount of research has been focused on the packing, mixing and sintering of binary powders. It is well known that if two powders having a size difference are mixed together that the mixture will have a higher density than that for either of the individual powders. In some cases a high density is desired solely for the green body use (e.g. nuclear fuel rods) or for the sintered body (e.g. refractories). The ultimate aim of studies on binary powders has been the development of materials which have superior properties over those obtained for either of the individual powders.

Packing

One of the primary objectives in the ceramics and powder metallurgy industries is the achievement of high green density bodies to minimize shrinkage and firing times on sintering. One of the approaches to this problem has been the mixing of two powders that have a large size

ratio ($\geq$10) in which case the finer component fills the interstices between the coarser particles.

In 1928, Furnas [1] analyzed theoretically the packing behavior of binary mixtures of this type and derived relations between the specific volume of a mixture and its composition. Two years later, Westman and Hugill [2] developed a graphical procedure based on the same concepts, apparently unaware of the earlier work of Furnas. In both of these presentations it was implicit in their arguments that the mixtures be homogeneous. In a number of studies [2-4] it was found that experimentally determined specific volumes do not exactly correspond to the theoretically predicted values. The reasons for these deviations have not been clearly established. One of the possible explanations for the discrepancy is that real binary powders are never perfectly mixed. Thus, the local compositions vary from position to position, and the local specific volumes vary correspondingly. The possibility of inhomogeneities is supported in a paper by Rhines [4], who detailed the occurrence of segregation in binary powder stacks and pointed out the natural instability of such a mixture.

In 1961 McGeary [3] attempted to obtain ideal particle packing by using a different packing technique. The procedure was to place the coarse particles into a container and vibrate it to its minimum volume. The finer constituent

was then placed on top of the coarse particle matrix and vibrated until the fines filtered through the particle stack. McGeary's results demonstrated that a discrepancy still existed between the experimental and theoretical values. It was stressed that the vibratory method was the only technique for obtaining high densities for binary mixtures of dry powders and that usual blending techniques were inferior for obtaining high densities. Nevertheless, it was not established why discrepancies existed between the theoretical and experimental values.

Sintering

Despite the recognized benefits of using binary mixtures of powders to increase the green density, few studies have centered on the sintering of binary mixtures that have a large size ratio. In 1969, O'Hara and Cutler [5] presented experimental results for the sintering kinetics of binary mixtures of alumina powders. Although they recognized the consequence of using binary powder mixtures that have large size differences, they did not differentiate the contributions to the shrinkage behavior from shrinkage stresses, compositional inhomogeneities, and fine to coarse particle contacts. In 1973 Coble [6] studied a square array of particles in which a fine particle just fits in the interstitial site and touches the coarse particles. His analysis demonstrated that increased shrinkage

can arise as a result of shrinkage stresses at the particle contacts. Onoda [7] used the Furnas model to account for the space-filling contributions of the coarse and fine components as they sintered. His analysis assumed that the coarse and fine components in a mixture sinter the same as a body of 100% of that component. While the model adequately explained some of the general trends of O'Hara and Cutler's data, there were some discrepancies at the intermediate compositions. One of the possibilities is that the sintered bodies were inhomogeneous.

Blending

It is generally recognized that compositional inhomogeneity is undesirable because it results in non-uniformity of the properties of the finished product. To obtain homogeneous mixtures, a variety of blending equipment has been developed to offset segregation. This equipment has been broadly classified [8, 9] according to the dominant mechanism of blending, which can be misleading and constitutes an over-simplification of the blending process. In fact, little is understood about the fundamental nature of the blending process or the interaction of mechanisms during blending. Indeed, control of segregation in blending equipment has been based on observation and experience instead of from an understanding of the fundamental aspects of powder blending.

Research Plan

From the above discussion it is seen that compositional inhomogeneities are an important fact at all levels of powder processing. The elimination of them and the understanding of their role in property determination is of major importance. The research presented here represents an effort to approach powder processing from a fundamental viewpoint.

In Chapter II a theoretical procedure for determining the specific volume of an inhomogeneous binary mixture having a large radius ratio is presented. The procedure is based upon the hypothesis that the Furnas model holds on a local level. The methodology developed is demonstrated using two hypothetical compositional distribution functions. In one case the compositional distribution describes changes that take place from a completely unmixed to a completely mixed state. The second utilizes the normal distribution for describing smaller compositional variations. It is seen that the results from the hypothetical examples are similar to those presented in the literature.

The objective of Chapter III was to determine whether the bulk specific volume of inhomogeneous binary powder mixtures, having a large size ratio, correspond to the theoretical values calculated from known compositional

inhomogeneity data, as derived in Chapter II. This represents a test of whether the Furnas model is valid locally. To minimize the effects of particle geometry, experiments were performed with glass microbeads.

In Chapter IV Onoda's analysis of the sintering of binary mixtures is extended to include the effects of compositional inhomogeneities. The theoretical shrinkage equations are presented and a hypothetical example is given that assumes the compositional variation of a reasonably well-mixed body is described by the normal distribution. The results of the calculation of the volumetric shrinkage for inhomogeneous mixtures are compared to those obtained from the original sintering model for an ideally mixed body.

Chapter V involves a fundamental description of particle blending which focuses on the interrelationships between particle dynamics and the energetics of the blending process. The principles are incorporated into an analysis of the vibratory blending process. To test the general validity of the fundamental processes of blending, a series of experiments were performed. In these experiments parameters such as the frequency of vibration, container size, particle size ratio and particle size distribution were chosen to test specific fundamental aspects of the blending process.

CHAPTER II

INHOMOGENEITY-PACKING DENSITY RELATIONS IN BINARY POWDERS

Introduction

The packing density of two-component powder mixtures, where one component has a much different particle size than the other, was first analyzed theoretically by Furnas [1], who derived relations between the specific volume of a mixture and composition, using simple space-filling concepts. In subsequent packing studies [2, 3, 4], the experimental values for specific volume of mixtures were shown in most cases to deviate significantly from the ideal values predicted by the Furnas model. The reasons for these deviations have not been clearly established. A major problem in identifying the causes for the discrepancy between experiment and theory is that no method has been available to determine which of the assumptions of the Furnas model are inappropriate for real systems.

One of the possible explanations for the discrepancy is that real binary powders are never perfectly mixed. The local compositions vary from position to position, and the local specific volumes vary correspondingly.

Accepting the reality of compositional variations, the question arises as to whether the overall specific volume of a real mixture could be accounted for by assuming that the Furnas model is valid locally. To test this hypothesis on real powders, a methodology must be developed which facilitates the calculation of the overall specific volume from compositional variation characteristics. Validity of the hypothesis for any given experimental mixture may be tested by comparing measured specific volumes with the calculated values obtained by measuring compositional characteristics.

In the present paper, a theoretical procedure is developed for calculating specific volumes of binary mixtures from compositional inhomogeneity characteristics, assuming that the Furnas model applies locally. The compositional characteristics needed for the calculation are identified.

This methodology is demonstrated with two compositional distribution functions that serve as examples of pertinent functions for powder mixing. The first function describes the compositional distribution changes that occur in a horizontal drum mixer when two powders are mixed from a completely unmixed to a completely mixed state. The second is a normal (Gaussian) distribution which is useful for describing smaller variations from perfect mixing such as occur in the final mixing stage.

These examples provide some insight into what can be expected for the relations between the specific volume of mixtures when compositional variations are the only cause for deviations from the original Furnas equation.

The Furnas Theory

Furnas [1] derived relations between the specific volume and composition of ideal binary mixtures. He used the partial specific volumes of the coarse and fine components to elucidate the concepts and to show a simple graphic procedure for representing the relations. Westman and Hugill [2] proposed the same graphic procedure, apparently unaware of the earlier work. The mathematical equations were rederived by Rose and Robinson [11].

From the fundamental theorem of partial differentiation, the specific volume (v) of a binary mixture can be expressed by

$$v = \bar{v}_c w_c + \bar{v}_f w_f \qquad (1)$$

where w_c and w_f are the weight fractions and $\bar{v}_c$ and $\bar{v}_f$ are the partial specific volumes of the coarse and fine components. The partial specific volumes are defined as

$$\bar{v}_c \equiv \left[\frac{\partial V}{\partial W_c}\right]_{W_f}$$

$$\bar{v}_f \equiv \left[\frac{\partial V}{\partial W_f}\right]_{W_c}$$

where V is the total volume of the mixture and W_c and W_f are the weight of the coarse and fine components. The partial specific volume of a component can be viewed as the volume increase experienced by a mixture of a given composition when a unit weight of the component is added to a very large quantity of the mixture.

Furnas stated that the compositional range for mixtures can be divided into two regions (Figure 1). In region I, the overall volume is controlled by the quantity of coarse component; the fine component occupies the void spaces between the coarse particles and does not add to the overall volume. Therefore, throughout region I, $\bar{v}_f = 0$ and $\bar{v}_c = v_c$, the specific volume of the 100% coarse composition. Equation (1) becomes

$$\text{region I:} \quad v_I = v_c w_c = v_c\ (1 - w_f) \qquad (2)$$

where the subscript I refers to region I.

In region II, the mixture can be visualized as a matrix of packed fine component containing isolated coarse

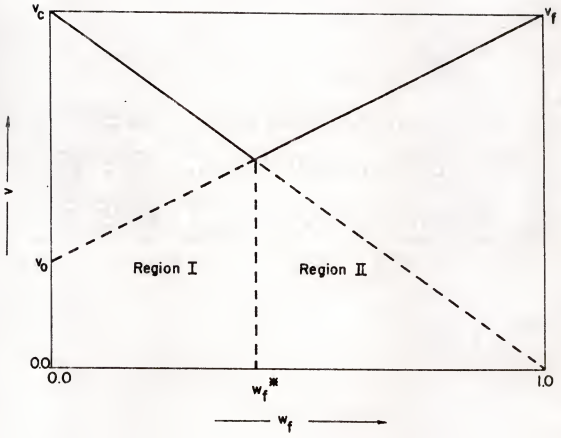

Figure 1. Theoretical binary packing relations of Furnas.

particles imbedded in the matrix. Adding more fine component simply adds more matrix. Thus the partial specific volume of the fine component is equal to that of the 100% fine composition, v_f. Adding more coarse component increases the volume by the solid volume of the particles, so $\bar{v}_c$ equals v_o, the true specific volume of the materials. Equation (1) becomes

$$\text{region II:} \quad v_{II} = v_o w_c + v_f w_f$$

$$= v_o + (v_f - v_o) w_f \qquad (3)$$

where the subscript II refers to region II.

The boundary between regions I and II is obtained by setting $v_I = v_{II}$ (Equations (2) and (3)) and solving for w_f. The result is

$$w_f^* = \frac{v_c - v_o}{v_f + v_c - v_o} \qquad (4)$$

where w_f^* is the boundary composition. At this composition, the fine particles completely fill the voids between packed coarse particles, and the addition of more fine component would expand the coarse particle bed if perfectly mixed.

The basic assumption of the Furnas model can be stated succinctly as:

$$\left.\begin{aligned}\bar{v}_c &= v_c \\ \bar{v}_f &= 0\end{aligned}\right\} \quad \text{for } 0 \leq w_f \leq w_f^*$$

$$\left.\begin{aligned}\bar{v}_c &= v_o \\ \bar{v}_f &= v_f\end{aligned}\right\} \quad \text{for } w_f^* \leq w_f \leq 1$$

Discrepancies between experimental values of v and the Furnas predictions must be due to the breakdown of one or more of these assumptions.

Local Compositional Variations and Specific Volume

Compositional variations within a body can be represented by a continuous frequency function, $f(w_f)$, which can be estimated experimentally by extracting numerous small samples from the body and measuring the composition of each sample. The frequency function is defined so that the probability of a small sample having a composition between a and b is given by

$$\int_a^b f(w_f)dw_f$$

Over the entire compositional range (a = 0, b = 1), the integral would be unity.

The overall (average) composition ($\tilde{w}_f$) of the body is given by

$$\tilde{w}_f = \int_0^1 w_f f(w_f)\, dw_f$$

It is useful to divide the entire population of samples into two compositional regions (regions I and II). These regions are the same as those defined previously, with w_f^* being the dividing boundary. In particular, we are interested in the proportion (by weight) of samples in each region (the proportions being designated as q_I and q_{II}), with their sum equaling unity and in the average compositions, $(\tilde{w}_f)_I$ and $(\tilde{w}_f)_{II}$, of these samples. The values of q_I, q_{II}, $(\tilde{w}_f)_I$, and $(\tilde{w}_f)_{II}$ can be calculated for a continuous frequency function, $f(w_f)$, as:

$$q_I = \int_0^{w_f^*} f(w_f)\, dw_f \tag{5}$$

$$q_{II} = \int_{w_f^*}^1 f(w_f)\, dw_f \tag{6}$$

$$(\tilde{w}_f)_I = \frac{\int_0^{w_f^*} w_f\, f(w_f)\, dw_f}{\int_0^{w_f^*} f(w_f)\, dw_f} \tag{7}$$

$$(\tilde{w}_f)_{II} = \frac{\int_{w_f^*}^1 w_f\, f(w_f)\, dw_f}{\int_{w_f^*}^1 f(w_f)\, dw_f} \tag{8}$$

From these equations, it can be seen that

$$(q_I)(\tilde{w}_f)_I = \int_0^{w_f^*} w_f \, f(w_f) \, dw_f \tag{9}$$

$$(q_{II})(\tilde{w}_f)_{II} = \int_{w_f^*}^{1} w_f \, f(w_f) \, dw_f \tag{10}$$

and

$$\tilde{w}_f = (q_I)(\tilde{w}_f)_I + (q_{II})(\tilde{w}_f)_{II} \tag{11}$$

Theorem

If every incremental mass element of a binary mixture has a specific volume consistent with its local composition according to the Furnas equations, the specific volume, $\hat{v}$, of the overall body is given by

$$\hat{v} = q_I \tilde{v}_I + q_{II} \tilde{v}_{II} \tag{12}$$

where q_I and q_{II} are the proportions by weight of elements in regions I and II, respectively, and $\tilde{v}_I$ and $\tilde{v}_{II}$ are the Furnas specific volumes corresponding to $(\tilde{w}_f)_I$ and $(\tilde{w}_f)_{II}$, the average compositions of elements in regions I and II.

Proof

The total volume (V) of a body is equal to the summation of the volumes of individual elements, given by $W\int_0^1 v\, f(w_f)\, dw_f$ where W is the total weight. The specific volume, $\hat{v}$, of the body is therefore

$$\hat{v} = \frac{V}{W} = \int_0^1 v\, f(w_f)\, dw_f$$

The function $\hat{v}$ is the specific volume as calculated by the Furnas equations and therefore follows different relations for regions I and II (Equations (2) and (3)). The integral in the above equation can be separated into two integrals

$$\hat{v} = \int_0^{w_f^*} v_I\, f(w_f)\, dw_f + \int_{w_f^*}^1 v_{II}\, f(w_f)\, dw_f$$

Substituting the expressions for v_I and v_{II} from Equations (2) and (3):

$$\hat{v} = v_c \int_0^{w_f^*} f(w_f)\, dw_f - v_c \int_0^{w_f^*} w_f\, f(w_f)\, dw_f +$$

$$v_o \int_{w_f^*}^1 f(w_f)\, dw_f + (v_f - v_o) \int_{w_f^*}^1 w_f\, f(w_f)\, dw_f$$

Using the relations expressed in Equations (5) to (8) these equations become

$$\hat{v} = v_c q_I - v_c q_I (\tilde{w}_f)_I + v_o q_{II} + (v_f - v_o) q_{II} (\tilde{w}_f)_{II}$$

$$= q_I [v_c - v_c (\tilde{w}_f)_I] + q_{II} [v_o + (v_f - v_o)(\tilde{w}_f)_{II}]$$

$$= q_I \tilde{v}_I + q_{II} \tilde{v}_{II} \qquad (13)$$

which proves the theorem.

The Continuous Cumulative Frequency Function

From the preceding theoretical considerations, $\hat{v}$ can be determined (for the localized Furnas model) if one of the following sets of parameters is known:

$$[\tilde{w}_f, (\tilde{w}_f)_I, (\tilde{w}_f)_{II}];$$

or

$$[\tilde{w}_f, (\tilde{w}_f)_I \text{ or } (\tilde{w}_f)_{II}, q_I \text{ or } q_{II}]$$

Calculating $(\tilde{w}_f)_I$, $(\tilde{w}_f)_{II}$, q_I, and q_{II} depends on having a frequency function $f(w_f)$ to perform the integrations given in Equations (5) to (8).

In some circumstances it is convenient to use a cumulative frequency function rather than the frequency function. The previous equations may also be used to calculate the parameters for such a cumulative frequency

function. The most common procedure for characterizing the compositional variations in a body is to introduce a thief probe which removes small samples from different parts of the mixture; the composition of each of these is evaluated. From these data, a curve can be constructed for Q, the cumulative weight fraction of all samples having compositions less than w_f, versus w_f. The slope S of this curve at any point is

$$S = \left[\frac{dQ}{dw_f}\right]_{w_f}$$

where dQ is the weight fraction in the interval dw_f at composition w_f. This is equivalent to the probability of finding a sample in the same compositional intervals, dw_f. Therefore,

$$f(w_f)\ dw_f = S\ dw_f = dQ$$

which shows that the continuous frequency function is equal to the slope S measured from the experimental data.

Equations (5) to (8) become

$$q_I = \int_0^{Q^*} dQ = Q^* \tag{14}$$

$$q_{II} = \int_{Q^*}^{1} dQ = 1 - Q^* \tag{15}$$

$$(\tilde{w}_f)_I = \frac{1}{q_I} \int_o^{Q^*} w_f dQ \tag{16}$$

$$(\tilde{w}_f)_{II} = \frac{1}{q_{II}} \int_{Q^*}^{1} w_f dQ \tag{17}$$

where Q^* is the value of Q corresponding to w_f^*. The integrals in Equations (16) and (17) represent the areas under the curve where w_f is the ordinate and Q is the abscissa within the designated limits for Q. This is shown schematically in Figure 2, where area $A_I = (\tilde{w}_f)_I q_I$ and area $A_{II} = (\tilde{w}_f)_{II} q_{II}$.

The Degree of Mixedness Parameter

Two empirical relations between bulk density and a mixedness parameter M have been proposed, where M is defined [10] as

$$M = 1 - \frac{\sigma}{\sigma_o} \tag{18}$$

where σ is the experimentally determined standard deviation of the compositional variation around the average composition for the mixture and σ_o is the theoretical standard deviation for a completely unmixed batch. Rose and Robinson [11] proposed the relation

$$\delta = \delta_U + 0.7\ M\ (\delta_M - \delta_U) \tag{19}$$

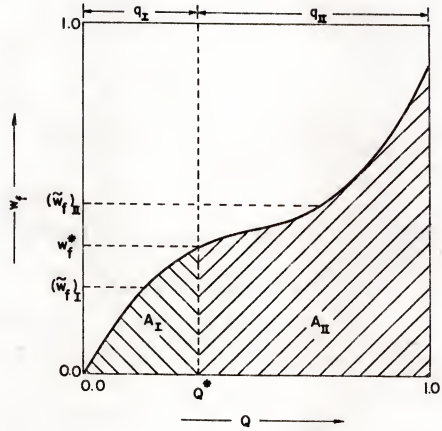

Figure 2. Schematic integration areas for calculating $(\tilde{w}_f)_I$ and $(\tilde{w}_f)_{II}$ from w_f-Q data.

where δ, δ_U, and δ_M are the bulk densities of the real mixtures, a fully unmixed system, and an ideally mixed system, respectively. Fuerstenau and Fouladi [12] proposed the equation

$$\delta = \delta_U + M^2(\delta_M - \delta_U) \tag{20}$$

For both cases, the equations imply that the bulk density should be uniquely related to M. Since the two investigators found different dependencies of δ on M, and since the mixing and sampling procedures were entirely different, the existence of a generally valid, unique relationship between δ and M remains in question.

For all possible distributions, there cannot exist a unique, single-valued relation between $\hat{v}$ and σ if the localized Furnas model is obeyed. Since M is a function of σ, this would also show that $\hat{v}$ and M are also not uniquely related for all possible variations.

From Equations (11) and (13), and the fact that $q_I + q_{II} = 1$, we can combine these equations to yield

$$\hat{v} = \left[\frac{\tilde{w}_f - (\tilde{w}_f)_{II}}{(\tilde{w}_f)_I - (\tilde{w}_f)_{II}}\right]\left[v_c - v_c(\tilde{w}_f)_I\right] + \left[v_o + (v_f - v_o)(\tilde{w}_f)_{II}\right] \tag{21}$$

This shows that $\hat{v}$ can be expressed in terms of the variables $\tilde{w}_f$, $(\tilde{w}_f)_I$, and $(\tilde{w}_f)_{II}$ only.

It can be demonstrated [13] that the overall variance σ^2 of a frequency distribution which has been subdivided into two populations is related to the means and variances of these populations by

$$\sigma^2 = q_I \sigma_I^2 + q_{II} \sigma_{II}^2 + q_I \left[(\tilde{w}_f)_I - \tilde{w}_f\right]^2 + q_{II} \left[(\tilde{w}_f)_{II} - \tilde{w}_f\right]^2 \qquad (22)$$

where σ_I and σ_{II} are the standard deviations of the populations in regions I and II, respectively.

That $\hat{v}$ and σ are not uniquely related for all distributions can be shown by considering a given set of parameters: $\tilde{w}_f'$, $(\tilde{w}_f)_I'$, and $(\tilde{w}_f)_{II}'$. These values uniquely fix $\hat{v}$ by Equation (13). However, these values do not fix a unique value for σ^2 according to Equation (22). The last two terms of Equation (22) are fixed, but σ_I^2 and σ_{II}^2 are not fixed. Many distributions within region I can give the same $(\tilde{w}_f)_I$ but may have different σ_I values. Consequently, σ can be any value, depending on σ_I and σ_{II}, under conditions where $\hat{v}$ is fixed by constant values of $\tilde{w}_f$, $(\tilde{w}_f)_I$, and $(\tilde{w}_f)_{II}$. Thus, no unique relation exists between $\hat{v}$ and σ for all possible variations.

However, special cases may be found where $\hat{v}$ and σ would be related uniquely. If a specific continuous frequency function, such as a normal distribution curve, describes all of the variations that can exist in the body, then σ_I, σ_{II}, $(\tilde{w}_f)_I$ and $(\tilde{w}_f)_{II}$ would be completely fixed for a given $\tilde{w}_f$ and σ. Single-value relations between σ and $\hat{v}$ would therefore result. Similar arguments would be valid for most types of distribution curves as long as the type of function remains the same for all variations. Despite the shortcoming of characterizing the degree of mixedness of a powder with the parameter M, it is informative to model the change in the specific volume during mixing by assuming a hypothetical case in which M is uniquely defined.

Hypothetical Examples

Specific Volume Changes With Mixing From M = 0 to M = 1

To monitor the change in mixing of a binary powder from the unmixed to the mixed state, a relation between the change in the compositional variation and the level of mixing is required. It must represent low degrees of mixing when the compositional distribution is skewed and high degrees of mixing when the distribution is uniform. For illustration the compositional distribution change can be modeled using a diffusion analogy [10].

In the mixing literature some models are presented [10, 14, 15] to characterize the course of mixing based on a diffusion analogy. Of these, the equation given by Lacey [10] fulfills the stated criteria and is simple to manipulate mathematically. Therefore, it was chosen to illustrate this case. Lacey's equation is

$$w_f = \frac{2}{\pi} \sum_{p=1}^{p=\infty} e^{-q^2 \pi T} \frac{\sin p \tilde{w}_f \pi}{p} \cdot \cos px\pi + \tilde{w}_f \qquad (23)$$

where $\tilde{w}_f$ is the average weight fraction of the finer component, w_f is the weight fraction of the finer component at any fractional position x in the mixer, T is a diffusion-mixer constant, and p is an integer. The compositional variation described by this equation is shown in Figure 3 at various degrees of mixing.

The form of this equation is such that the compositional variation is a function of the position in a mixer. The calculation of q_I, q_{II}, $(\tilde{w}_f)_I$ and $(\tilde{w}_f)_{II}$ is facilitated by changing the form of the above equation into a form expressed in terms of Q. To make this transformation, w_f was calculated for every 0.01 increment in x. Using these values of w_f, the specific volume was calculated for each volume element, assuming the Furnas relations. If the level of the mixer is equal for all positions, each of the elements has an equal volume and the weight of

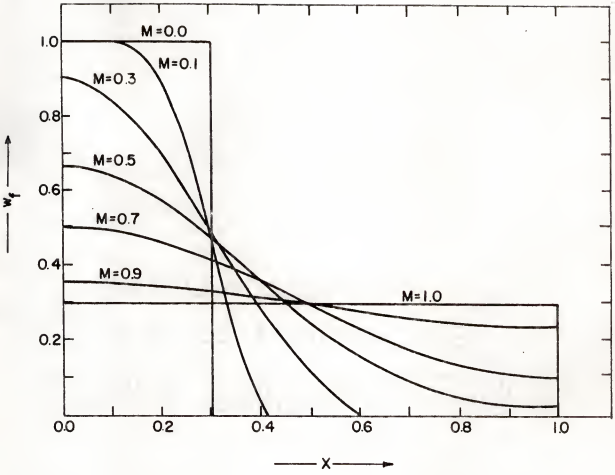

Figure 3. Theoretical compositional variations with increased mixing in a horizontal mixer.

these elements can be calculated; with this information the function Q can be constructed. Applying Equations (14) through (17) to Q, the specific volume can be calculated for any average composition and degree of mixing.

Figure 4 shows a specific volume versus average composition curve for various constant degrees of mixing based on the above calculations. For high degrees of mixing there is no deviation from the Furnas relations except when $\tilde{w}_f$ is near w_f^*. These deviations correspond to the compositional distribution overlapping both regions I and II. When there is no overlapping, the specific volume is the same as that calculated from the Furnas relations (i.e. $q_I = 0$ or $q_{II} = 0$). Therefore, the criteria of the Furnas model may be met even when the degree of mixing is less than one, except near w_f^*. For example, if $\tilde{w}_f = 0.7$, then to fulfill the Furnas model only a mixedness number of 0.4 is required. Thus, the greater the average compositional deviation from w_f^*, the greater is the possibility of attaining the maximum density of the binary mixture.

The Normal Distribution

A simple means to characterize a reasonably well-mixed binary powder (i.e. having a small compositional variation) is the use of the normal distribution, which describes relatively well the compositional variation in

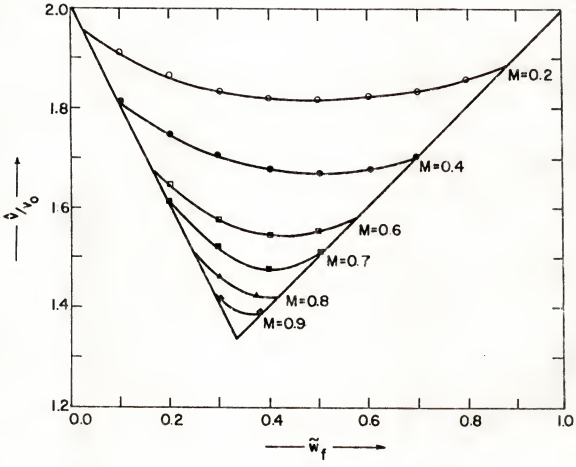

Figure 4. The calculated specific volume, $\hat{v}$, normalized by the theoretical volume, v_0, of the particles, at various levels of mixing, assuming the Lacey distribution.

the later stages of mixing [15, 16]. The normal distribution is given by

$$f(w_f) = \frac{1}{\sigma\sqrt{2\pi}} e^{-1/2 \left[\frac{w_f - \tilde{w}_f}{\sigma}\right]^2} \quad (24)$$

where σ is the standard deviation and w_f and $\tilde{w}_f$ are as defined previously.

Using the above calculations, small deviations from the Furnas equations due to compositional inhomogeneities can be plotted. Using the normal distribution below a mixedness number of $\sim$0.7 leads to errors due to the truncation of one side of the distribution; thus the distribution is no longer truly normal. Therefore, the normal distribution will be used only if truncation is held to a minimum. As a result, the curves do not span the entire compositional range because of truncation at low $\tilde{w}_f$ values and low degrees of mixing. The results of these calculations are shown in Figure 5.

In general, observations on Figure 4 are also true for the normal distribution. If the deviations of the two curves are compared at common degrees of mixedness, for M = 0.9 the deviations appear the same since Equation (23) can be approximated by the normal distribution at high degrees of mixing (i.e. $M \geq 0.9$), but at lower mixing levels (i.e. $M < 0.9$) the compositional distributions are

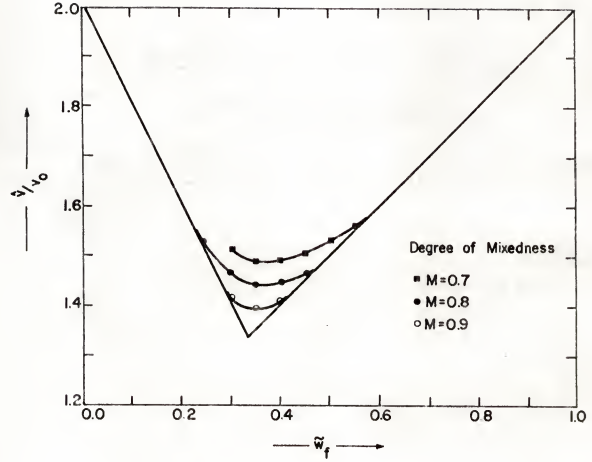

Figure 5. The calculated specific volume, $\hat{v}$, normalized by the theoretical volume, v_0, of the particles, at various levels of mixing, assuming the normal distribution.

different; therefore, the calculated specific volumes will be different.

Discussion and Summary

A relatively simple procedure for calculating the specific volume of a mixture, assuming the Furnas model is valid locally, has been developed. Experimentally, the simplest approach is to obtain a cumulative weight fraction curve for the compositional variations. This curve can be integrated by numerical methods to obtain the necessary parameters for calculating the specific volume.

It has been demonstrated that, generally, no unique relations can exist between $\dot{v}$ and $\ddot{M}$, but that special cases exist if the change in compositional variation follows well-defined relations. Figure 6 plots bulk density versus the degree of mixedness for the two hypothetical distributions, as well as the proposed empirical relations of Rose and Robinson [11] and Fuerstenau and Fouladi [12]. Neither relation approximates the theoretical data calculated from the hypothetical distributions, possibly because both relations are based on empirical data in which the change in the compositional distribution was different from that for the hypothetical cases. Also, the proposed relations may be unique only to the experimental conditions under which the data were collected.

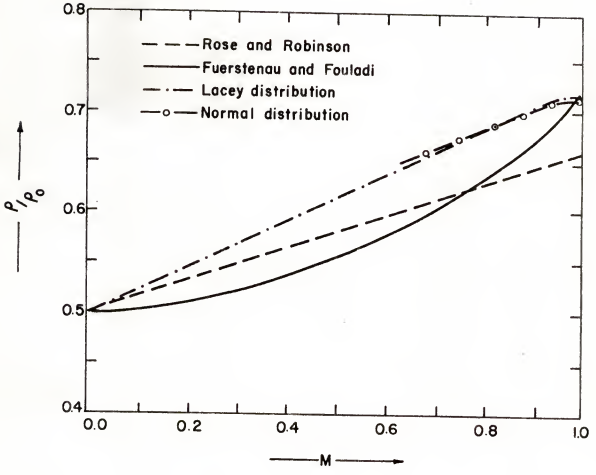

Figure 6. Comparison of the hypothetical data and two proposed relationships for the effect of mixing on the bulk density at $\bar{w}_f = 0.3$.

The specific volume-composition curves calculated by the proposed methodology have shapes resembling typical experimental data found by many previous investigators. This fact does not prove that the Furnas model is valid on a local scale, however. Experiments are needed in which both specific volume and compositional variations are measured as a function of average composition. The experimental specific volumes could then be compared with those calculated from the compositional variation data, thereby testing directly the hypothesis that the local regions obey the Furnas model. If discrepancies occur, the magnitude of the variation can be used to study other factors (e.g. agglomeration) that may contribute to lower specific volumes.

CHAPTER III

INHOMOGENEITY-PACKING DENSITY RELATIONS IN BINARY POWDERS--EXPERIMENTAL STUDIES

Introduction

In the previous chapter, a methodology was presented that makes it possible to calculate the specific volume of mixtures when compositional inhomogeneities exist. The assumption was made that the Furnas theory adequately predicts the specific volume for a small volume element, and the overall specific volume is calculated by summing up the contributions of every volume element in the body. If the compositional variations in a body are known, a specific volume can be calculated.

The purpose of the present investigation was to determine whether the specific volumes of imperfectly mixed binary powders correspond to the theoretical values calculated from known compositional inhomogeneity data. For these initial studies, spherical glass beads*, all of the same chemical composition, were utilized to minimize other complicating effects due to particle geometry.

*Microbeads, Cataphote, Inc., Jackson, Mississippi.

To test the model two different types of mixtures were analyzed. In one, the compositional variation was constrained to one dimension to facilitate the sampling process. In the other, the compositional variation is "random" in all three dimensions such as would occur in a typical mixing process.

After being mixed the particle mixtures were sampled and a cumulative weight fraction finer than w_f versus w_f curve (i.e. Q) determined. The local Furnas specific volume ($\hat{v}$) was calculated after the integration of the curve with the use of Equations (14) to (17). The theoretical specific volume was then compared to the bulk specific volume to test the local Furnas model.

One-Dimensional Packing

Experimental Procedure

To obtain mixtures having a gradient in composition predominantly in one direction, binary mixtures of glass beads having a size ratio of 18:1 were mixed in a specially-designed sampling container (Figure 7). The container, 6.35 cm. in diameter, was filled to a height of ∿17 cm. with -20+30 mesh (-841+595μ) glass beads. A fine powder of -325+400 mesh (-44+37μ) glass beads was placed on top of the coarse beads so that the average weight fraction of fine particles in the mixture was either 0.323 or 0.254.

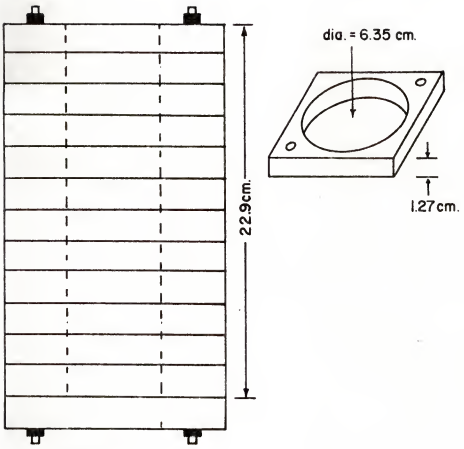

Figure 7. Sampling container for analysis of one-dimensional compositional variation.

Each powder stack was vibrated for various times so that different levels of mixedness could be obtained. The vibration was provided by an unbalanced wheel which was powered by a 0.005 horsepower, 60 cycle motor that was attached to a spring-supported table. After vibration the bulk specific volume (v_B) was determined by measuring the height of the stack in the container and calculating the volume of the mixture, which was then divided by the total weight of the powder.

To characterize the mixture as a function of the height, the container consisted of a series of 13 to 18 plexiglass rings which could be removed one section at a time. The powder that was contained in each section was sieved to determine the composition of the mixture at that level of the container.

To better estimate the level of inhomogeneity in a stack, a continuous cumulative distribution curve is determined from the experimental data in the following manner. First, the weight fraction of powder in each section is determined by dividing the weight of powder in the section by the total weight of the mixture. Beginning with the top of the stack, the composition as a function of the height of the stack is determined by adding the weight fractions obtained for each section. This procedure is possible because the composition varies continuously with depth. The data are then plotted versus w_f, as demonstrated

in the example shown in Figure 8. To approximate a continuous distribution function, it is assumed that the composition (w_f) obtained for a section is the composition at the middle of that section, which makes it possible to estimate the compositional distribution function by joining the midpoints of each increment by a straight line. To obtain a Q versus w_f curve from this plot, the elements are rearranged so that w_f decreases monotonically or is constant for the entire range of cumulative weight fractions (i.e. from 0 to 1.0). Then, the value of q_I and q_{II} can be determined directly from the Q value corresponding to w_f^*. Values for $(\hat{w}_f)_I$ and $(\hat{w}_f)_{II}$ are obtained by numerical integration (using Equations (16) and (17)) of the Q curves.

By using the above procedure, it is assumed that the compositional variations in the horizontal direction are small compared with the variations in the vertical direction. If the compositional variation in any layer is confined to either region I or II, the theory has shown that the specific volume is that predicted by the Furnas equation for the average compositional of that region. Large errors may result if the variation extends between two regions (across w_f^*).

Results and Discussion

The curves in Figures 9 and 10 show the experimentally determined composition versus cumulative weight fraction

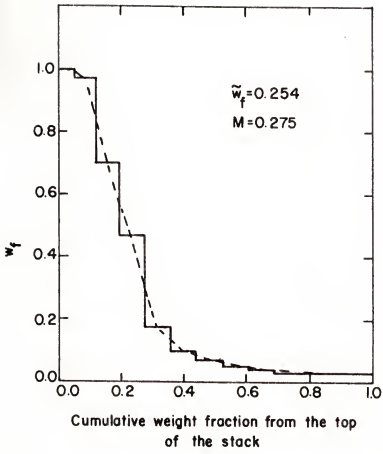

Figure 8. Compositional distribution curve for $\tilde{w}_f$ = 0.254 with M = 0.275 for one-dimensional compositional variation.

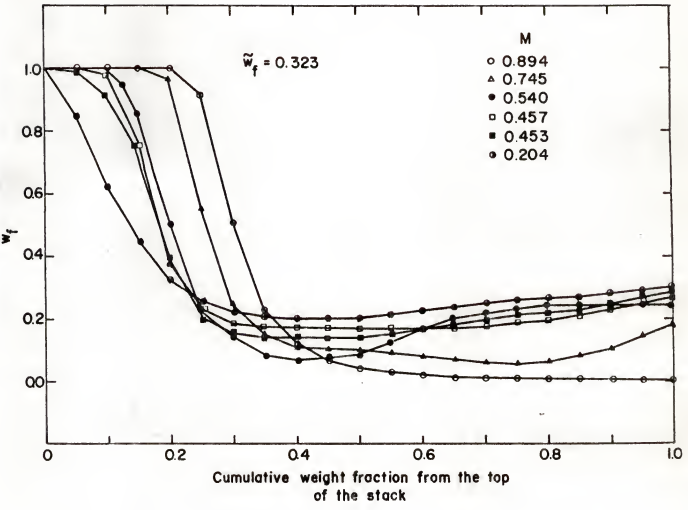

Figure 9. Experimental w_f versus cumulative weight fraction from the top of the stack curves for $\tilde{w}_f$ = 0.323 and for one-dimensional compositional variation.

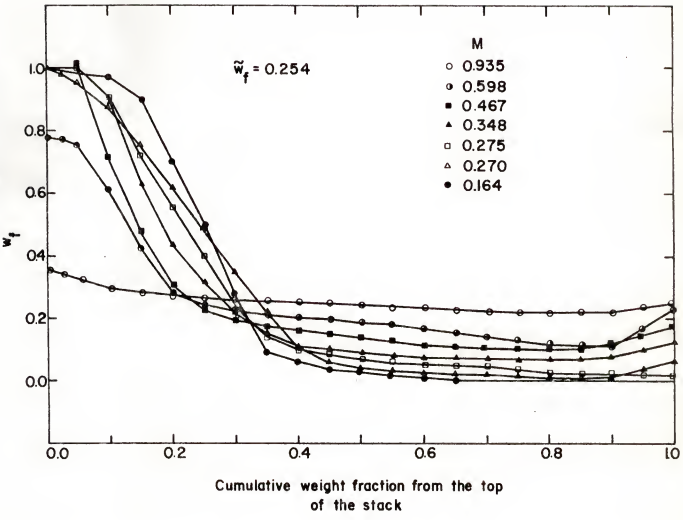

Figure 10. Experimental w_f versus cumulative weight fraction from the top of the stack curves for $\tilde{w}_f = 0.254$ and for one-dimensional compositional variation.

from the top of the stack for different degrees of mixing (M) for the compositions $\tilde{w}_f = 0.323$ and $\tilde{w}_f = 0.254$. A comparison of the actual, calculated and the Furnas specific volumes is indicated in Figure 11.

These results indicate that in general a high level of agreement exists between the predicted specific volume ($\hat{v}$) and the actual bulk specific volume at all levels of inhomogeneity. This agreement can be better appreciated by calculating the percentage of the discrepancy (accounted for by the new model) between the actual specific volume and that predicted by the original Furnas model. The average percentage of discrepancy accounted for at average compositions of 0.323 and 0.254 is 98% and 92%, respectively. In a few mixtures, the predicted specific volume is greater than the bulk specific volume (although by less than 1%). This deviation might be a result of an error in the estimate of the compositional distribution near w_f^* as explained previously, but in this case the small deviation is within the experimental error of our measurements. In general, the level of agreement indicates that the local Furnas model satisfactorily explains the discrepancies due to inhomogeneities for the one-dimensional stacking conditions of our experiments.

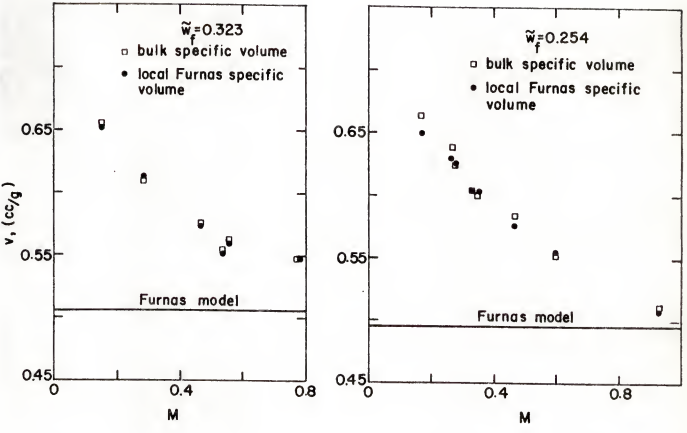

Figure 11. The Furnas, the experimental and local Furnas specific volumes versus the mixedness parameter for $\tilde{w}_f$ equal to 0.323 and 0.254.

Three-Dimensional Packings

Since real powder mixtures typically have compositional variations in three dimensions, attempts were made to analyze the specific volumes of bodies with such variations. Interest was focused on relatively small compositional variations (i.e. M values of 0.77 to 0.96) which typify the values obtained in real mixers.

Experimental Procedure

Two glass bead powders, -30+40 mesh and -325+400 mesh (a 13:1 average size ratio), were hand mixed until they appeared to be homogeneous. The mixture was then transferred to a sampling box (Figure 12) and vibrated on a vibrating table until a minimum stack volume was attained. The volume was measured and divided by the total weight which gives the specific volume of the mixture. A thief probe, shown schematically in Figure 12, is inserted horizontally into each hole (which is normally closed with a rubber stopper) while light pressure is applied to the top of the powder to hold it in place. By rotating the outer jacket of the probe, five 0.1cc chambers are opened to the powder at 2 cm. lengths of the probe. In this manner 75 point samples were taken for each mixture. The samples withdrawn with the thief were sieved on small screens to determine their composition.

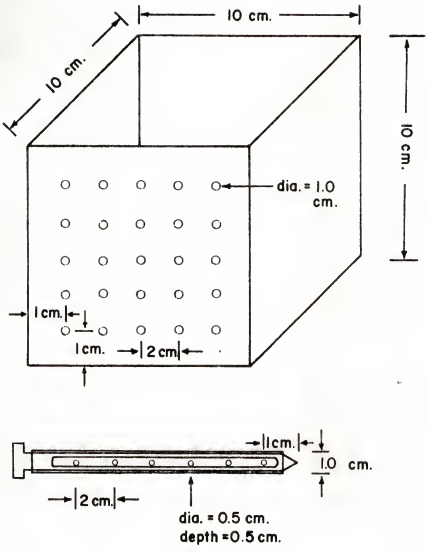

Figure 12. Sampling container and thief sampler for analyzing three-dimensional compositional variation.

Results and Discussion

Compositions of 0.150, 0.254 and 0.325 which lie in region II, at w_f^* and in region I, respectively were studied. The Q versus w_f curves obtained by the sampling are given in Figures 13 and 14. The 100% fine and 100% coarse powders vibrated in the box had specific volumes, $v_f = 0.725$ and $v_c = 0.664$. From this procedure theoretical specific volumes ($\hat{v}$) can be calculated. In Tables I and II, the $\hat{v}$ values are compared with the actual specific volumes (v_B) for various compositions. Several mixtures for each composition were analyzed to show the variations in M that occur by the mixing procedure and the corresponding variations in v_B and $\hat{v}$. A perfect agreement (within experimental accuracy) between v_B and $\hat{v}$ was found for the compositions 0.15 and 0.325, while significant discrepancies were found for $\tilde{w}_f = 0.254$.

As shown in Figure 14, the compositions of all samples taken from the 0.150 composition mixture were in region I. Similarly, those of the 0.325 composition mixtures were entirely in region II. The fact that $\hat{v}$ agreed with v_B for these mixtures even though M was not unity is consistent with the localized Furnas model prediction for cases where the sample populations are all within one region.

For the mixtures where $\tilde{w}_f = 0.254$, agreement between $\hat{v}$ and v_B was not perfect, but the difference was much less than that between v_B and the Furnas specific volume

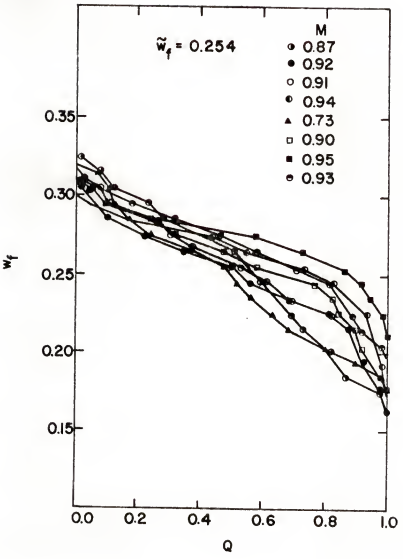

Figure 13. Experimental compositional variation curves for $\tilde{w}_f$ = 0.254.

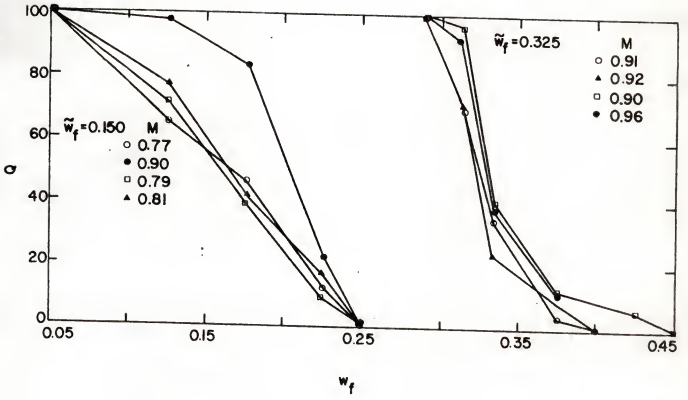

Figure 14. Experimental compositional variation curves for $\tilde{w}_f$ = 0.150 and 0.325.

Table I

$\tilde{w}_f = 0.325$			$\tilde{w}_f = 0.150$		
v_B	$v=\hat{v}$	M	v_B	$v=\hat{v}$	M
0.512	0.512	0.91	0.564	0.564	0.77
0.512	0.512	0.92	0.564	0.564	0.90
0.512	0.512	0.90	0.564	0.564	0.79
0.512	0.512	0.96	0.564	0.564	0.81

Experimental and theoretical specific volumes for three-dimensional compositional variations for $\tilde{w}_f$ equal to 0.325 and 0.150.

Table II

$\tilde{w}_f = 0.254$			
v_B	$\hat{v}$	M	%
0.508	0.513	0.87	---
0.513	0.507	0.92	65
0.506	0.506	0.91	100
0.510	0.503	0.94	50
0.513	0.512	0.73	94
0.514	0.506	0.90	56
0.513	0.507	0.95	65
0.515	0.509	0.93	68
		Avg. % =	71

Experimental and theoretical specific volumes for three-dimensional compositional variations for $\tilde{w}_f$ equal to 0.254 (w_f^*).

(0.496 cc/g). Table II shows that an average of 71% of the discrepancy between v_B and the specific volume calculated from the original Furnas model is accounted for by the localized Furnas model. It is conceivable (although not proven) that the remaining discrepancy is a result of experimental error because not enough samples were taken to adequately characterize the compositional variation. This is supported by the observation that some segregation of powder occurred at the container walls. The sampling probe did not take samples next to the walls, consequently, the ends of the distribution curve were probably underestimated. A broader distribution would have resulted in the calculation of a higher $\hat{v}$, which would have more closely approached v_B.

Summary

The results of the experiments indicate that binary mixtures of glass beads, having a radius ratio of 13:1 or higher, follow Furnas packing on a local scale, and the specific volumes of mixtures deviate from the original Furnas predictions because of local compositional inhomogeneities.

It remains to be seen whether powders which have irregularly-shaped particles or a smaller particle size ratio would also follow the localized Furnas model when

using very fine particles which do not pack regularly due to agglomeration. Thus, the basic assumptions of the model may be invalidated and lead to incorrect predictions of specific volume. The usefulness of the present study is that the effects of additional variables to the packing volumes can be better recognized, because contributions due to inhomogeneities can be determined.

CHAPTER IV

THE SINTERING OF INHOMOGENEOUS BINARY POWER MIXTURES

Introduction

Recently a geometrical model [7] was presented to describe the sintering behavior of binary powder mixtures that have large particle size ratios (i.e. $\geq$10). The model is based on the theoretical relations for the calculation of the specific volume of a binary powder mixture as given by Furnas [1] and assumes homogeneous mixtures. Since real powder mixtures are seldom homogeneous, it is necessary to extend the Furnas relations to make allowances for compositional variations in the sintering model.

In Chapter II a methodology was developed which makes possible the calculation of the specific volume of an inhomogeneous body. In this chapter the methodology is incorporated into the ideal sintering model to permit the calculation of the shrinkage during sintering for an inhomogeneous body. The shrinkage behavior is demonstrated with a hypothetical case in which two separate sintering conditions are considered. In one case only the fines are assumed to sinter, while in the other both powders are

assumed to sinter with the fines sintering at a faster rate than the coarse component. For the calculation of the volumetric shrinkage the level of inhomogeneity is modeled for a well-mixed body by assuming the compositional variation is described by the normal distribution. The results of these calculations are compared to those obtained from the original sintering model for an ideally mixed body.

Theory

As a first-order approximation, Onoda first assumed the Furnas relations would hold throughout sintering for a binary powder mixture. It was also assumed that the fine and coarse powders in the mixture sintered the same as 100% of that component and that there was no contribution to the shrinkage from fine to coarse particle contacts. To simulate sintering, the partial specific volumes of the coarse and fine powders were decreased as they would in sintering and the change in the overall specific volume calculated. The volumetric shrinkage can be calculated in the following manner:

$$\frac{\Delta V}{V} = \frac{\hat{v} - \hat{v}'}{\hat{v}} \tag{25}$$

where ΔV is the change in volume due to shrinkage, V is the initial volume of the stack, $\hat{v}$ is the theoretical specific volume given for the initial particle stack and

v' is the theoretical specific volume after sintering. To analyze the shrinkage for the inhomogeneous mixture, it is informative to first consider the homogeneous case.

Fines Sintering Only

The first case considered is that of a homogeneous body which is characterized by sintering of the fines and no sintering of the coarse. Conceptually, three types of shrinkage behavior are classified according to compositions for these sintering conditions. For composition of $w_f \leq w_f^*$ the coarse particles form a matrix with the fines in the interstitial sites between the coarse particles. In the absence of coarse particles sintering, the fines sinter locally in the interstitial sites. This results in changes of the interstitial pore geometry but no shrinkage of the mixture. When $w_f \geq w_f^*$, the mixture is composed of coarse particles interspersed in a matrix of fine particles. When sintered, the mixture shrinks until fully dense or until the coarse particles are brought into contact as a result of the shrinkage of the fines. This configuration is then similar to a coarse particle matrix in that no further shrinkage occurs. This event is represented by a characteristic composition which is given by

$$w_{f_s}^m = \frac{v_c - v_o}{v_f' + v_c - v_o} \tag{26}$$

where v_f' is the partial specific volume of the fines after sintering. This composition is similar to w_f^* in that it is

the boundary composition between the two relations for sintering. The composition $w_{f_s}^m$, changes continuously with sintering from w_f^* for the initial stack to w_f^m when the fines have completely densified (i.e. $v_f' = v_o$). This composition is given by

$$w_f^m = \frac{v_c - v_o}{v_c} \tag{27}$$

and represents the mixture that completely densifies under these conditions with the minimum amount of shrinkage. That is, the fines will sinter to 100% density just at the moment the coarse particles come into contact. The compositional influence can be divided into two composition ranges for $w_f \geq w_f^*$. But, if $w_{f_s}^m \leq w_f \leq 1.0$, the coarse particles do not come into contact on sintering and thus do not directly influence the sintering of the fines. If $w_f^* \leq w_f \leq w_{f_s}^m$, the fines shrink until constrained by coarse particles coming into contact.

Quantitatively, the volumetric shrinkage for the compositional range, $w_{f_s}^m \leq w_f \leq 1.0$, is given by substituting Equation (3) into Equation (25) giving

$$\frac{\Delta V}{V} = \frac{w_f (v_f - v_f')}{v_o + w_f (v_f - v_o)} \tag{28}$$

If w_f lies between w_f^* and $w_{f_s}^m$ then the total shrinkage is given in the following manner:

$$\frac{\Delta V}{V} = \frac{[v_o + (v_f - v_o)\, w_f] - [v_c\,(1 - w_f)]}{v_o + (v_f - v_o)\, w_f}$$

because $\hat{v}' = v_c\,(1 - w_f)$ which is the final specific volume. The above relation between the bulk shrinkage and composition is not linear, as was incorrectly supposed in the original paper [7]. This is seen in Figure 15 where the ideal relations for the volumetric shrinkage are plotted for various levels of sintering.

For the case of a powder mixture that has compositional inhomogeneities, a single composition does not adequately describe the mixture. Instead, a compositional distribution and <u>average</u> composition ($\tilde{w}_f$) are required. To calculate the volumetric shrinkage of an inhomogeneous body, Equation (12) is substituted into Equation (25) giving

$$\frac{\Delta V}{V} = \frac{(q_I \tilde{v}_I + q_{II} \tilde{v}_{II}) - (q_I' \tilde{v}_I' + q_{II}' \tilde{v}_{II}')}{q_I \tilde{v}_I + q_{II} \tilde{v}_{II}} \qquad (29)$$

where the prime designates the parameters after sintering. The values of q_I and q_{II} are altered during sintering because the value of v_f' decreases and thus $w_{f_s}^m$ changes. That is, the boundary composition which delineates the size of q_I and q_{II} changes from w_f^* to $w_{f_s}^m$. For an inhomogeneous body, $w_{f_s}^m$ is the boundary composition above which all the volume elements can still sinter, but below which there is no further shrinkage. Therefore, as $w_{f_s}^m$ increases

the amount of material that is able to shrink with further sintering will decrease (i.e. q_{II} decreases).

Equation (29) simplifies to the relation given for a homogeneous body when w_f lies between $w_{f_s}^m$ and 1.0. This is because the compositional variation is contained entirely between $w_{f_s}^m$ and 1.0, thus $q_I = 0$. Likewise, if the compositional variation is restricted to region I, no shrinkage of the body occurs.

In Figure 15, the shrinkage behavior is plotted for various stages of sintering as a function of the average weight fraction of fines for M = 1.0 (ideal) and M = 0.85. The dashed lines represent the theoretical shrinkage assuming the compositional variation for a well-mixed body can be described by the normal distribution, which is given by Equation (24).

The level of inhomogeneity has no geometric influence on the sintering behavior for compositional ranges where either $\tilde{w}_f > 0.6$ or $\tilde{w}_f < 0.2$. That is, for $\tilde{w}_f > 0.6$, the coarse particles are evenly dispersed in the matrix of fines and do not come into contact on sintering. For $\tilde{w}_f < 0.2$, the fines are merely set in the coarse interstitial voids and are only able to sinter locally.

The total volumetric shrinkage is less than ideal for inhomogeneous bodies with compositions between w_f^* and w_f^m. This is accounted for by a fraction of the volume elements having compositions less than w_f^*, in which case there is

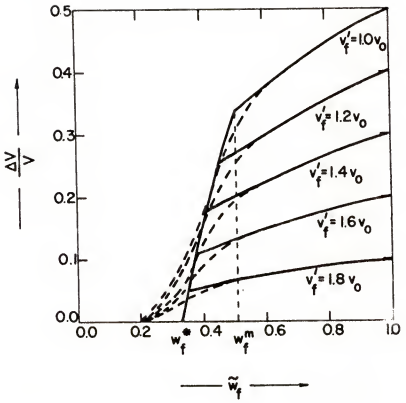

Figure 15. The relative shrinkage of binary mixtures at various levels of sintering for two levels of homogeneity when only the fines sinter.

no shrinkage. For a body with $\tilde{w}_f$ less than w_f^*, shrinkage occurs because a small proportion of the body has a composition greater than w_f^* and is able to partially shrink upon sintering.

In Figure 16 the bulk shrinkage for $\tilde{w}_f = 0.5$ and 0.4 is plotted as a function of the specific volume of the fines (v_f') for two levels of mixing. It is generally observed that the overall shrinkage is less than ideal and is dependent upon the relative position of the average composition to w_f^* and w_f^m. For example, the difference in shrinkage behavior caused by inhomogeneities is maximized at $v_f' = 1.5\ v_o$ for $\tilde{w}_f = 0.4$, but for $\tilde{w}_f = 0.5$, the maximum discrepancy occurs at $v_f' = 1.0\ v_o$. Thus, the influence of compositional variation emerges at different stages of sintering for different compositions.

Coarse and Fines Sintering

Consider the shrinkage of a homogeneous body in which there is simultaneous sintering of the coarse and fine powders. The shrinkage behavior can be classified by the same three compositional ranges as used for the case of fines sintering only. The compositional ranges are again determined by w_f^* and $w_{f_s}^m$ (Equations (4) and (26)). Conceptually, the sintering behavior is similar to the case of the fines sintering only, except that the mixture continues to shrink when the coarse particles are brought into contact.

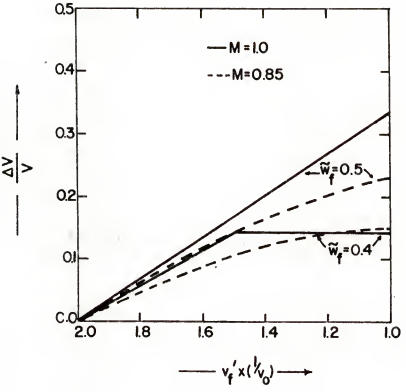

Figure 16. The relative shrinkage during sintering for two average compositions and two levels of homogeneity when only the fines sinter.

The shrinkage for compositions between $w_{f_s}^m$ and 1.0 is simply given by Equation (28) as the coarse particles do not influence the sintering of the fines. If the composition lies between zero and w_f^*, the shrinkage is due only to sintering of the coarse particles and is given by

$$\frac{\Delta V}{V} = \frac{v_c\ (1 - w_f) - v_c'\ (1 - w_f)}{v_c\ (1 - w_f)} \tag{30}$$

The shrinkage is composition independent for the early stages of sintering until the coarse particles sinter sufficiently to eliminate their interstitial porosity (i.e. when $v_c'\ (1 - w_f) = v_o$). This first occurs at w_f^*. The total shrinkage is thus given by

$$\frac{\Delta V}{V} = \frac{v_c'\ (1 - w_f) - v_o}{v_c'\ (1 - w_f)} \tag{31}$$

The significance of w_f^* is that it is the composition at which the minimum degree of shrinkage is required for complete densification.

The shrinkage for compositions between w_f^* and $w_{f_s}^m$ is illustrated by considering a simple example. In Figure 17 the specific volume after shrinkage is plotted as a function of composition for the sintering of the individual powders. For the composition w_f^* the coarse particles are in contact so that sintering proceeds as the rate of shrinkage of the coarse component. For bodies with the compositon $w_{f_s}^m$, the change in specific volume is due only to the sintering of

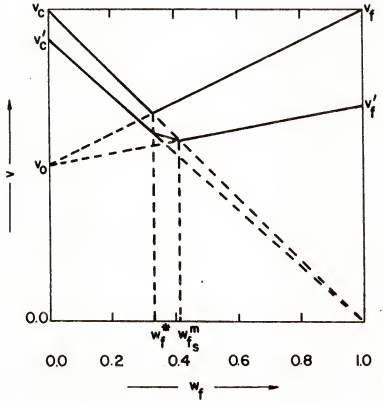

Figure 17. Hypothetical sintered volumes for compositions between w_f^* and $w_{f_s}^m$, assuming a linear relation.

the fines until the coarse particles are brought into contact. Therefore, at intermediate compositions between these two limits the degree of shrinkage involves intermediate sintering rates of the coarse between that at w_f^* and that for initial sintering at $w_{f_s}^m$. Without prior knowledge of the sintering rates it is not possible to calculate the degree of shrinkage. For illustrative purposes, it is assumed that the relation for the sintered specific volume is linear between w_f^* and $w_{f_s}^m$. To calculate the hypothetical sintering behavior, the relative change in the specific volume of the fine component was taken to be five times that of the coarse component. For example, as v_c' changes from a value of 2.0 v_o to 1.96 v_o, v_f' decreases from 2.0 v_o to 1.8 v_o. The hypothetical shrinkage behavior is given in Figure 18.

For inhomogeneous binary mixtures, a general equation is not possible due to the shrinkage in intermediate composition. For the extremes in average composition, when either q_I or $q_{II} = 0$, the shrinkage is given by Equation (28) for large $\tilde{w}_f$ and by Equation (30) for small $\tilde{w}_f$. To calculate the sintered specific volume of an inhomogeneous mixture, it is necessary to determine the quantity and average compositional ranges. This is done in a manner similar to that used for the case of the fines sintering only. The specific volume of the inhomogeneous body after sintering is then given by

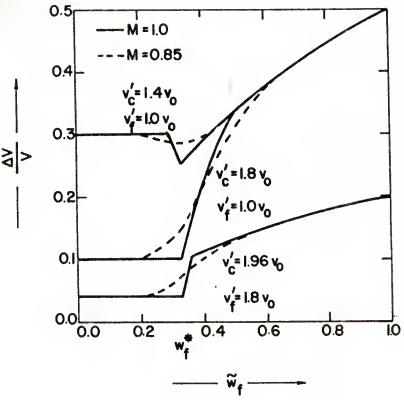

Figure 18. The relative shrinkage for fines sintering faster than the coarse particles for three stages of sintering and two levels of homogeneity.

$$\hat{v}' = \tilde{v}_I' q_I' + \tilde{v}_{II}' q_{II}' + \tilde{v}_{III}' q_{III}' \qquad (32)$$

where $\tilde{v}_I'$, $\tilde{v}_{II}'$, $\tilde{v}_{III}'$ are the Furnas specific volumes corresponding to $\tilde{w}_{f_I}$, $\tilde{w}_{f_{II}}$ and $\tilde{w}_{f_{III}}$, the average compositions of elements in regions I, II and III. The regions are $0 \leq \tilde{w}_{f_I} \leq w_f^*$, $w_f^* \leq \tilde{w}_{f_{II}} \leq w_{f_s}^m$ and $w_{f_s}^m \leq \tilde{w}_{f_{III}} \leq 1.0$. Using the same assumptions as for sintering of homogeneous mixtures, the degree of shrinkage was calculated for three stages of sintering. The results are plotted in Figure 18 as a function of the average composition of the mixture.

The deviation in shrinkage from that for the ideal case changes progressively with sintering for a body that has a composition slightly greater than w_f^*. Due to the spread in composition, a volume fraction of the mixture has compositions less than w_f^*. Therefore, in the initial stages of sintering (e.g. $v_c' = 1.96\ v_o$, $v_f' = 1.8\ v_o$) the degree of shrinkage is less than ideal because these volume elements sinter minimally in comparison to the ideal composition, which is controlled by the sintering of the fines. With the eventual sintering of the coarse particles (e.g. $v_f' = 1.0\ v_o$, $v_c' = 1.4\ v_o$) the shrinkage of the inhomogeneous mixture is greater than the shrinkage for the homogeneous case. This is attributed to those volume elements, which have a composition less than w_f^*, having to shrink more for complete densification than if all the volume elements had the same composition (i.e. ideal mixing).

This behavior is seen more clearly in Figure 19 where the shrinkage is plotted as a function of v_c' for average compositions of 0.35 and 0.45. It is apparent that the shrinkage behavior is dependent on the relative position of the average composition to w_f^* (0.33). For example, the shrinkage curve for $\tilde{w}_f = 0.35$ shows greater shrinkage in the later stages of sintering for the inhomogeneous body than the ideal mixture (by the previous argument), whereas, there is less shrinkage than the ideal for the same conditions at an average composition of 0.45.

Another aspect of composition is its control over the rate of sintering. That is, by the time $v_c' = 1.8\ v_o$ the composition 0.45 has almost completely densified, but for the composition 0.35 to approach the same relative degree of densification sintering needs to progress to $v_c' = 1.6\ v_o$. Nevertheless, in this case, both compositions must sinter a longer period of time than the ideal mixture to eliminate porosity between the coarse particles.

Another consequence of the average composition being near w_f^* is that "irregular" shrinkage behavior occurs, as seen in Figure 19 for $\tilde{w}_f = 0.35$ and M = 1.0. The "irregularity" is due to shrinkage being controlled first by sintering of the fines and later by the sintering of the coarse particles. Thus, there is an appreciable change in the sintering rate and a commensurate change in the slope. Although this also occurs for the inhomogeneous

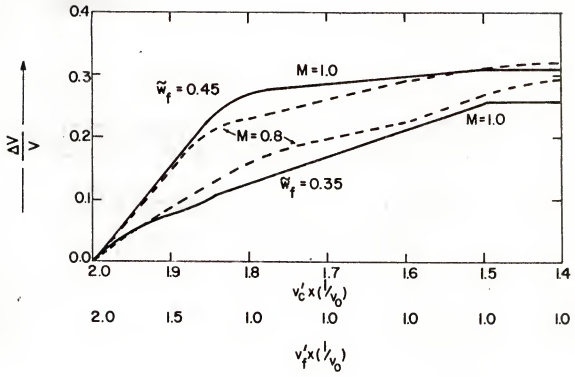

Figure 19. The relative shrinkage as a function of the change in the specific volumes of the fine and coarse particles for three stages of sintering and two levels of homogeneity.

mixtures, the inhomogeneity masks this behavior because its shrinkage is dependent on a broad range of compositions instead of a single composition.

Discussion of Results

In 1969 O'Hara and Cutler [5] presented results from a study of the kinetics of sintering for binary mixtures of alumina powders. Onoda analyzed [7] some of their data but found discrepancies that were unexplained with the ideal sintering model. To determine whether these discrepancies could be explained by compositional inhomogeneities, O'Hara and Cutler's data for powder mixtures having a nominal size ratio of 14 (3-6μ and 53-74μ) were replotted (Figure 20). The dashed line for $t^{0.46} = 24.6$ is an extrapolation of the trend in the data and is similar to the model prediction. By comparing Figures 18 and 20 for the initial stages of sintering some general statements about the sintering model can be made.

The experimental curve generally displays the same features as predicted by the theoretical model for non-homogeneous mixtures. There is no noticeable effect of the fines on the shrinkage behavior of the coarse particles at low values of $\tilde{w}_f$ for $t^{0.46} = 7.9$ and a transition region exists that smoothly changes through the intermediate compositions. The sintering behavior for the intermediate compositions suggests that the sintered bodies are inhomogeneous.

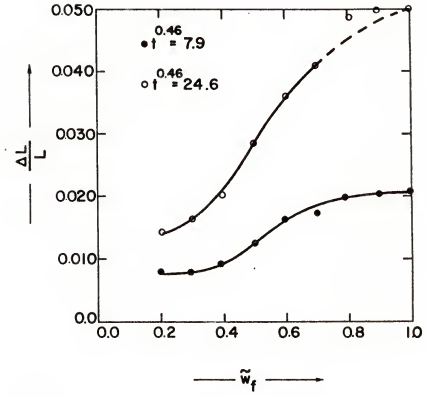

Figure 20. Experimental data of O'Hara and Cutler [5] for the relative linear shrinkage for different compositions after two constant sintering times (minutes).

At high values of $\tilde{w}_f$ (i.e. ≥ 0.8) there is a discrepancy between what would be expected theoretically (dashed line) and what is found experimentally. For compositions in this range, the theory predicts that the degree of shrinkage should be less than that for 100% fines, whereas the data shows the degree of shrinkage to be nearly the same. Further data [5] is given which demonstrates that the rate of shrinkage of the binary mixture at $\tilde{w}_f = 0.8$ is nearly the same as that for the 100% fines, suggesting that the body undergoes enhanced sintering. This behavior can be interpreted to be a result of stresses in the body which may be due to inhomogeneities or the influence of fines sintering to coarse particles.

It has been shown [6] theoretically that stresses can arise due to the sintering of fine to coarse particles. In this case, stresses may have enhanced the sintering of the binary mixtures, whereas in other cases stresses may result in reduced sintering. With the data available it is not possible to discern the true nature of these "discrepancies."

In an inhomogeneous body, stresses and/or defects may arise between nearly adjacent volume elements that have the same composition but which are separated by a lower density region. Theoretically, regions with a greater amount of fine particles will sinter faster than regions having a lower w_f. Upon sintering, these regions will

shrink away from the lower density regions giving rise to stresses that may result in the fracture of particle contacts in the lower density region. Depending on the degree of inhomogeneity, this type of shrinkage behavior could lead to the development of macro-voids on a local scale, thus lowering the overall properties of the body.

From this model two compositions (w_f^* and w_f^m) are noted that have particular practical importance. At the composition w_f^* the minimum shrinkage is realized for a body having the geometry of a binary mixture. To achieve a high density at this composition both the fine and coarse particles must sinter. Thus, the time involved to achieve full density is dependent upon the rate of shrinkage of the coarse particles. The composition w_f^m represents a body that undergoes the minimum degree of shrinkage if only the fines sinter. Theoretically, full density is attained for a body with this composition if the fines sinter fully. If we take the composition w_f^m (0.5) and note its shrinkage for the case of the full sintering of the fines and the partial sintering of the coarse (i.e. $v_f' = v_o$, $v_c' = 1.8\ v_o$) in Figure 18, it is observed that full density (theoretical) is not achieved. This is due to the incomplete sintering of those volume elements that have compositions less than w_f^m. Thus a composition slightly greater than w_f^m would be preferable under these conditions. The consequence of using a composition near w_f^m is that the time involved to attain

a high density is reduced in comparison to a body having a composition near w_f^*.

Summary

The sintering model does not directly incorporate any of the sintering mechanisms, except that the sintering behavior being considered undergoes shrinkage. This restricts the model to grain-boundary diffusion, volume diffusion, and viscous flow as mechanisms of sintering. Their influence is incorporated only in the behavior of the 100% coarse and fine components.

The importance of the model is that it is possible to recognize the effect of compositional inhomogeneities, the role of fine to coarse particle contacts and the geometrical contributions to the change in the specific volume of a binary powder mixture. The use of these equations in an analysis of the sintering behavior of binary powder mixtures could lead to a more fundamental understanding of the sintering behavior of powders that have continuous size distributions and/or local compositional inhomogeneities.

CHAPTER V

VIBRATORY BLENDING OF METAL POWDERS

Introduction

Despite the fact that the processes of powder blending and mixing have been practiced since antiquity there remains much that is not yet understood about the fundamental nature of these processes. According to ASTM [17], powder blending is defined as the thorough intermingling of powders of the same nominal composition, whereas powder mixing is defined as the thorough intermingling of powders of two or more materials. Commonly, segregation of the powder blend occurs during these processes, taking the form of a localized congregation of particles of a specific character. Segregation is undesirable, because it results in non-uniformity of the properties of the finished product. To offset segregation, a wide variety of types of blending equipment has been developed and used in the powder industries (e.g. powder metallurgy and ceramics).

Lacey [10] distinguishes two modes of particle blending which he calls, respectively, convective blending and diffusive blending. Convective blending is a stirring action, defined [10] as the transfer of adjacent groups of particles

from one location to another, as distinguished from particle by particle transport. Diffusive blending is defined [10] as the distribution of particles over a freshly developed surface of the powder blend. The main difference between these two mechanisms is that convection is the internal transport of clusters in the particle mass, while diffusive mixing requires an external surface of particles over which single particles can roll. The transfer of adjacent groups of particles past one another has been proposed as a separate mechanism (shear blending), but Hogg [18] asserts that it is simply an inevitable consequence of the operation of convective blending.

Blending equipment has been broadly classified [8,9] according to the predominant mechanism acting in the blending process. There are two rather different types of blenders that are thought to operate primarily by convection. One of these uses either vibratory motion or a rising air stream to activate the particle bed. In the other type, a convective action is generated by means of stirring paddles, or rotating augers. Examples of equipment in which the diffusive mechanism dominates are the V-blender and the drum mixer. It has been suggested [19-21] and, in fact, demonstrated [9, 22, 23] that blending equipment based on convective actions results in less segregation and a higher degree of homogeneity than does equipment of the diffusive type, when blending powders that have size differences.

The arbitrary classification of blending equipment according to its dominant mechanism of blending, however, can be misleading, in that it constitutes an over-simplification. In order to obtain a more fundamental view of the blending process it is enlightening to examine the behavior of single particles.

The Nature of Vibratory Blending

Principles

Consider one particle as it is situated in the powder mass before blending starts. Its relation to its immediate neighbors can be described in terms of its number of contacts with adjacent particles. The topological connectivity of the powder stack is defined mathematically as the total number of interparticle contacts in the mass minus the total number of particles plus one. This is a measure of the mechanical stability of the powder stack. The higher the connectivity of a given weight of powder the less likely is the powder to flow under mechanical impulse.

When a particle is added to a bed of powder,it is most likely to come to rest in contact with three supporting particles. Later, when more particles have been added to the bed, the reference particle will most often have three particles resting upon it from above. There are, thus, six particles making contact with the reference particle. Since each contact is shared between two particles,

the reference particle is considered to make three contacts with its neighbors. The particle is now held in position by other particles on all sides, a situation which may be contrasted with that of a surface particle, having but one and a half contacts and free to roll at the slightest disturbance. Where the powder is composed of particles of different sizes and shapes, there will be considerable variation in the number of contacts possessed by individual particles (comparable to their coordination number), with corresponding differences in the degree to which each is held in position in the powder stack.

Where all of the particles are essentially alike, their intermingling under mechanical impulse may be thought of as self-blending, a process which does essentially nothing to the nature of the powder mass. When particles of more than one size and shape are present, however, their motion may result in either an increase in the homogeneity of the mass, or in de-blending (i.e. segregation). Which dominates depends on the specific geometry of the particles and the nature of the mechanical agitation. Where a particle size difference exists, the smaller particles tend to have fewer contacts and, thus, to be more mobile. Very small particles, residing in openings between larger particles may have as few as one and one half contacts and be free to percolate down through the powder stack, under the influence of gravity, or minor mechanical

disturbance. Agitation of the stack tends to break contacts and open channels within the stack, further promoting percolation. This action tends to come to an end when the smaller particles have congregated at some lower stratum of the stack and have become locked in place by having three contact positions among particles of their own kind.

When the particle mass is given a sufficiently large mechanical impulse, it expands and some interparticle contacts are broken. For the top most layers of particles this impulse may give rise to their ejection from the surface. The movement of particles within the mass is restricted by surrounding particles. Each particle receives mechanical energy from its neighbors and distributes some of it to contacting neighbors, thus limiting its kinetic energy to the difference between that received and that transmitted. Toward the bottom of the stack the kinetic energy will be minimized because of the gravity loading by particles above. There will thus be a gradation from top to bottom wherein the upper most particles are in a state of fluidization and the bottom particles are largely bound in place.

In the lower portion of the particle mass the high connectivity (i.e. large average number of interparticle contacts) gives rise to movement by clusters or groups of particles. This results from the greater stability of

clusters of similar particles that constitute the inhomogeneity of the mass. Such clusters have a smaller probability of individual particle motion within them than the movement of the cluster with respect to other clusters. In other words, the system behaves as though made up of much larger bodies which themselves can receive and transmit the mechanical impulses. These clusters tend to flow in ribbon-like streams that circulate vertically within the powder mass. As each cluster reaches the upper portion of the stack it is able to retain more energy, which loosens it and tends to disperse its particles. Those particles that reach the top surface are totally disengaged from their former neighbors and the population of particles in this region becomes more homogeneous. Thus, the circulation of clusters brings the inhomogeneous matter to the active surface where true blending occurs.

As fluidized particles are recaptured by the main body,they may retain a homogeneous distribution which then becomes the blended state of the material. It is at this point in blending, however, that de-blending (segregation) by gravity may be initiated. In the presence of a sharp particle size difference, the smaller particles may drop through interstices in the stack, (i.e. percolate) particularly in the upper portion of the mass where the high kinetic energy maintains a low density of packing. In the extreme case the smaller particles may percolate

all the way through the stack and resegregate in its lower zones.

Observations

In the following discussion the previously described principles are incorporated with visual observations of the process to fundamentally characterize vibratory blending. With the addition of energy the stack expands and the particle mass is activated, creating a dynamic process of particle interaction in which the entire bed flows. The interaction of the flow and expansion of the bed is manifested in three generally defined blending zones (Figure 21). For descriptive purposes these zones are designated as the turbulent, high convective and low convective zones.

The turbulent zone exists only in the upper layers of the particle mass and is identified by a high kinetic energy per particle. The particles on the surface are continuously fluidized. Consequently, the average number of interparticle contacts per particle and the connectivity are low; varying between zero when particles are ejected and 1.5 when in contact with the surface. For a blend of like particles, self-blending is activated by a large number of interparticle collisions and, due to the freedom of movement, interdiffusion is easily accomplished. For the blending of particles that have size differences percolation occurs only on withdrawal of the mechanical

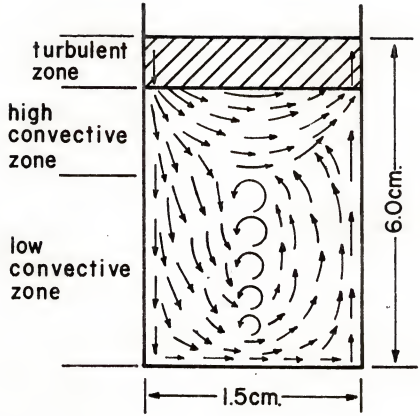

Figure 21. The flow pattern of a particle bed at a frequency of 2100 rpm, demonstrating the three main blending regimes.

energy, which gives rise to some segregation in the top surface layers of the stack.

Below the top few layers in the turbulent zone the particles are more constrained in their individual movement. This marks the incidence of the particle behavior which is characteristic of the high convective zone. In general, the high convective zone is partially expanded and has a high kinetic energy, although lower than that in the turbulent zone. The expansion results in a lower connectivity than for the original stack, which increases the probability for percolation of finer particles. Nevertheless, there are sufficient constraints on the particles that flow is characterized by clusters or groups of particles instead of individual particle behavior.

At a lower depth in the bed, which is designated the low convective zone, the degree of bed expansion is on the average less than that for the high convective zone. Consequently, the flow rate in this zone is considerably less than for the high convective zone. This region is characterized by a high average connectivity and flow by clusters of particles. In the initial stages of blending, clusters take the form of ribbons of the pure components of the blend and flow through the zone with little interpenetration. Because of the high connectivity of the zone, there is a lower probability for segregation.

From the above description, a general picture emerges for the vibratory blending process. That is, blending is

attained primarily in the turbulent zone by the diffusive mechanism and segregation is generally centered in the high convective zone because of its reduced connectivity. Although the low and high convective zones contribute little to the blending process per se, these zones enhance the overall process by transporting powder to the turbulent zone and by retaining the geometry of the blended mass after transport from the turbulent zone.

Experimental Procedure

Binary blends of atomized metal powders were used to test the proposed fundamental description of vibratory particle blending. The general procedure was to weigh out predetermined quantities of the two powders, totaling 28.5 grams, and to place them one on top of the other in a blending cylinder (Figure 22). The cylinder, which consists of a series of individual rings that are 1.25 centimeters in diameter and 0.64 centimeters tall, was filled to approximately 5 centimeters in height. The container was placed on a vibratory table and vibrated for a fixed period of time. After vibration, the container was taken apart section by section for compositional analysis and visual observations. In this manner it was possible to study specific contributions to vibratory blending by 1) the frequency of vibration, 2) the container size, 3) the particle size ratio, 4) the relative quantities of the

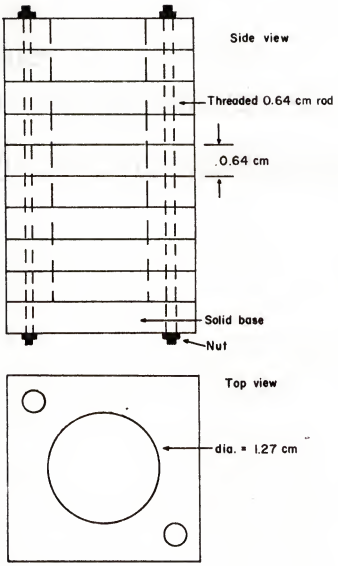

Figure 22. Blending container.

individual components in the blend (i.e. composition) and 5) the particle size distribution of the blend.

Powders

For these investigations it was desired to distinguish the two powders of the blend by color and size. To fulfill these criteria, atomized, high-purity, oxygen-free copper spheres and nickel carbonyl powders were used. The near identity of the densities of the two powders (Table III) provided freedom from density effects and the magnetism of the nickel permitted the complete separation of the powders for compositional analysis. The nickel and copper powders were divided into various sieve fractions (Table IV) to enable blending of samples having specific radius ratios. The radius ratio (R) is defined as the ratio of the average radius of the coarse component to the average radius of the fine component.

Blending

The powders were blended with a vibratory table (Figure 23) which is mounted on four soft springs (e). The blending container (a) was held off the table with the container holder (b). Vibration arises from the action of a rotating unbalanced wheel (d) that is powered by a 0.005 horsepower, 60 cycle motor (c). The frequency of the motor is controlled by a Powerstat variable autotransformer and the amplitude of vibration was maintained constant

Table III

Physical Characteristics of Powders

Parameter	Copper	Nickel
Density	8.90g/cc	8.94g/cc
Bulk Density	5.34g/cc	5.40g/cc
Flow Rate*	9.60g/sec	9.52g/sec
Magnetic	No	Yes

*Orifice diameter = 2mm.

Table IV

Sieve Mixtures for Different Radius Ratios

Radius Ratio	Copper	Nickel
1.0	-80+100	-80+100 (-177+149μ)
1.2	-80+100	-100+120 (-149+125μ)
1.4	-100+120	-140+170 (-105+88μ)
1.7	-80+100	-140+170
2.0	-80+100	-170+200 (-88+74μ)
2.4	-80+100	-200+230 (-74+63μ)
2.8	-80+100	-230+270 (-63+54μ)
4.4	-80+100	-325+400 (-44+37μ)

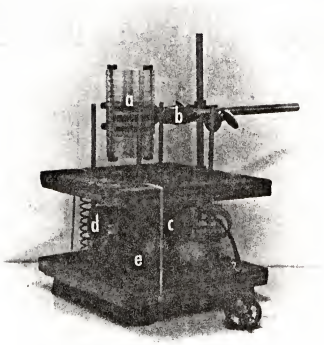

Figure 23. Photograph of blending apparatus showing a) blending container, b) container holder, c) motor, d) unbalanced wheel, and e) softspring.

(0.5mm vertical, 0.25mm horizontal). To damp out the low frequency vibrations rubber bands were fastened between the two levels of the vibratory table.

Characterization

To quantify the degree of blending, the cylindrical container was taken apart section by section. The powder contained within each section was magnetically separated and the amount of the two components determined by weighing, thus characterizing that section and position in the stack. Using the results from each section of the stack, the standard deviation (s) was calculated in the following manner:

$$s = \left[\sum_{i=1}^{n} \frac{(w_{Cu_i} - \bar{w}_{Cu})^2}{n - 1} \right]^{1/2}$$

where w_{Cu_i} is the weight fraction of copper in a section, $\bar{w}_{Cu}$ is the average weight fraction of copper in the blend (usually 0.5) and n is the number of sections used (i.e. 7). When s is high (i.e. > 0.10) the blend is obviously unblended with visual patches of the individual components present, and if s is low ($\leq$ 0.03) the body is well-blended with no visual evidence of segregation or clusters.

To judge differences of blending on a statistical basis, the F-test was applied at the 95% confidence level. The F-test is a statistical procedure whereby differences in data are inferred by comparing the variances of experiments. The F-test was utilized either on a sample for

sample basis or, if the variance (i.e. s^2) was not a function of the independent variable (i.e. time) for that set of conditions, they were tested as a group. Thus, each set of samples was characterized by the standard deviation and by visual observation, and differences were determined with the F-test.

Experimental Results

To obtain a general idea of the evolution of the homogenization process, binary mixtures of equi-sized particles were vibrated at 1800 rpm for a series of times. In Figure 24 the compositional variation in the upper section of the stack is minimal in comparison to that in the bottom half. The sharp break in the curves at section 12 is believed to be due to a relatively inactive spot that occurs where the direction of convective flow reverses in the low convective zone. The relatively small compositional variation in the top half of the stack demonstrates that blending is localized to the top half of the container and proceeds rapidly, whereas, the approach to the homogeneity in the bottom half is a relatively slow process. Thus it is concluded that blending per se is due primarily to the interaction between the high convective zone for rapid transport of powder to the turbulent zone, where the actual blending takes place. Although the low convective zone contributes no actual blending, the rate at which the

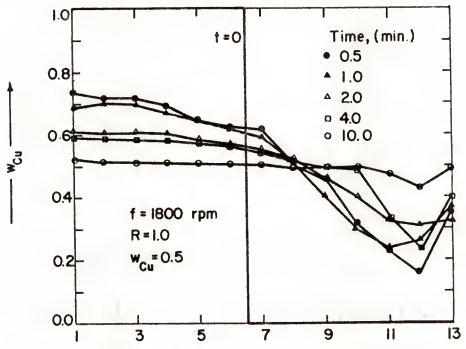

Figure 24. The change in the compositional distribution in the stack with progressive blending at 1800 rpm.

blend homogenizes is primarily dependent on this zone for the transport of particles to the upper zones.

Frequency of Vibration

As noted earlier, during vibration the degree of bed expansion depends on the energy input which gives rise to differences in the type of particle movement in the stack. To change the amount of energy delivered to the system the frequency was varied from 1600 to 2100 rpm for a duration of one to thirty minutes for blends of copper and nickel powders of the same particle size (-80+100 mesh).

The rate of blending in Figure 25 is minimal for low energies (f = 1600 and 1700 rpm) and rapid for high energies (f = 1800-2100 rpm). It was observed that only after thirty minutes of blending did the samples appear homogeneous for low energies. Visual observations of the process at these frequencies revealed that only convective zones existed. The blending that did occur at the low energies is attributed to transport over the top surface of the particle stack which gives rise to some intermingling. Samples at high energies (i.e. $\geq$ 1800 rpm) were all well-blended (except at t = 1 min.) and it was observed that the turbulent zone emerges at 1800 rpm. It is concluded that blending per se occurs at the turbulent zone and is necessary for the attainment of homogeneity.

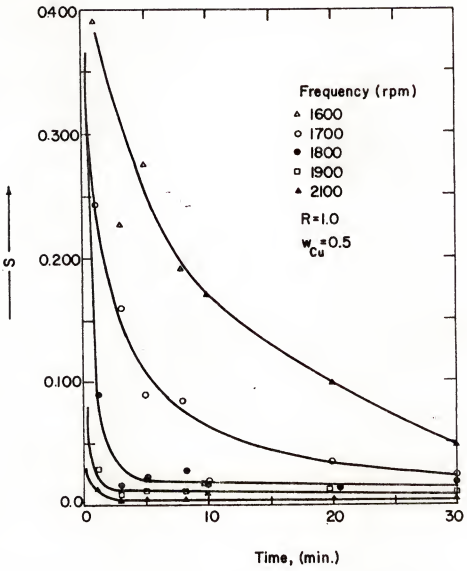

Figure 25. Time variation for blending at five different frequencies for a mixture having a radius ratio of 1.0.

Container Size

The size of the blending container is an important parameter because of its influence on the nature of the bed expansion. To determine this interrelationship three differently sized containers were used. The containers varied in physical dimension so that the height of the total sample was doubled for one comparison and in the other, the sample had the same height, but the diameter was doubled.

In Figure 26 the rate of blending is dependent on the height of the sample. This is because a higher proportion of the taller sample was transported by the low convective zone than for the shorter container. Thus, the powder flows at a slower rate than the powder in the high convective zone. Consequently, the transport of material to the turbulent zone is slower and must be transported a greater distance than for the shorter container. Also, these results demonstrate that blending is independent of the total weight of sample for these conditions.

Radius Ratio

Percolation decreases the attainable degree of homogeneity when there are size differences in a powder blend. To determine the influence of the size ratio on the percolation process, binary blends with size ratios of 1.0 to 2.8 (Table IV) were used. These samples were blended, beginning with the fine powder on top, for 30 minutes at

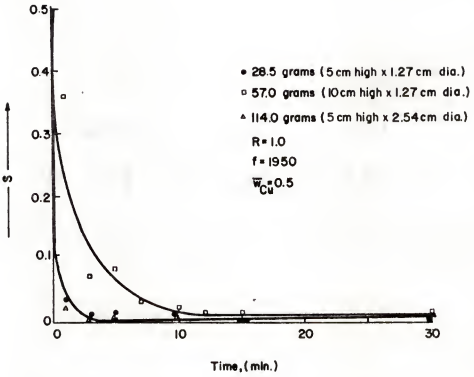

Figure 26. The rate of blending of a binary powder in three differently sized containers.

a frequency of 1950 rpm to attain the endpoint standard deviation. The weight fraction of the fines (w_f) for the experiments was 0.5.

None of the samples, except at R = 2.8, displayed definite bands of segregation although a thin layer of the coarse particles usually remained on the surface of the stack after vibration. Furthermore, although the stacks began with the fine component on top, the compositional distribution after blending revealed a gradient with the fines tending toward the bottom of the stack. In Figure 27 there is an initial drop in homogeneity between radius ratios of 1.0 to 1.4 and then a constant level of homogeneity from R = 1.4 to 2.4. The initial rise in s is attributed to the incidence of percolation due to size differences. The constant level of blending indicates for this range of size ratios that the overall process is more dependent on the energetics of the system than the geometrical relation between the coarse and fine powders. For a size ratio of 2.8 the rise in the standard deviation is attributed to the percolation of the fines to the bottom of the container. Indeed, this was confirmed by visual observation of the sampled stack in which a high concentration of fines was found in the bottom two sections. From observations of a blend having a size ratio of 4.4 (-80+100 mesh and -325+400 mesh) there was no interpenetration during blending and the powders segregated in the

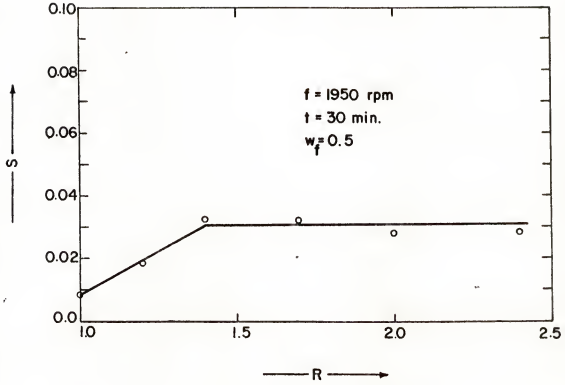

Figure 27. The degree of mixedness after thirty minutes of blending for various size ratios.

plane of flow instead of the horizontal plane. Therefore, these two size ratios (2.8 and 4.4) indicate the ∿limit for blending under these conditions.

Composition

To test the influence of the interparticle geometry on blending, two extremes in composition were vibrated (w_f = 0.1 and 0.9) for times of 1 to 30 minutes at a frequency of 2100 rpm. In Figure 28 the results are plotted with those for blends with a radius ratio of 1.0 and having the same initial composition.

The blending process for w_f = 0.1 is time dependent, whereas, that for w_f = 0.9 is time independent and gives the same standard deviation as obtained for R = 1.0. The result for w_f = 0.1 is a consequence of the slower transport of the fines to the turbulent zone, which arises because of the percolation of fines through channels in the coarse particle matrix during transport. For w_f = 0.9 there is no percolation because the fines form the matrix, which diminishes the possibility of coarse particles migrating through interstitial channels. It is noted that, in fact, these blends achieved the same degree of homogeneity as blends having no size differences. This is because the coarse particles are more stable (i.e. higher connectivity) when surrounded by fine particles instead of all coarse particles. Finally, the time independent part

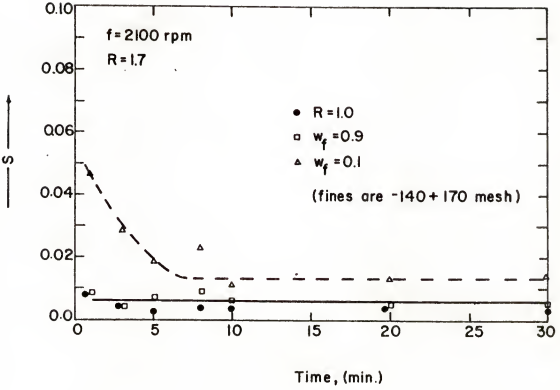

Figure 28. The rate of blending for binary mixtures with a size ratio of 1.7 at two different compositions (w_f = 0.1 and 0.9).

of the curve for $w_f = 0.9$ indicates that the blending and percolation processes are in "equilibrium." That is percolation and blending occur at the same rate.

Size Distribution

Usually, powders that are blended industrially have a wide size distribution instead of a narrow distribution. To determine whether a blend with a wide size distribution is susceptible to percolation, powders having a size distribution of -100+325 mesh were blended at a composition of 0.5 for a series of different times. These results are compared to blends that have a narrow size distribution (-80+100 mesh).

The general trend in Figure 29 demonstrates that the powders with the wider distribution blended slightly better than the other powder and with a more consistent degree of homogeneity. This is due to a more efficient utilization of the vibratory energy as a consequence of the higher connectivity of the blend.

To determine whether alteration of the channel size in the blend changes the percolation process, -100+325 mesh powder was used as the finer component for three binary compositions. By using a powder with a wider size distribution the interparticle geometry is changed as a result of the variety of sizes in the blend. Because these particles can pack together in a variety of ways the interparticle channel size is correspondingly changing

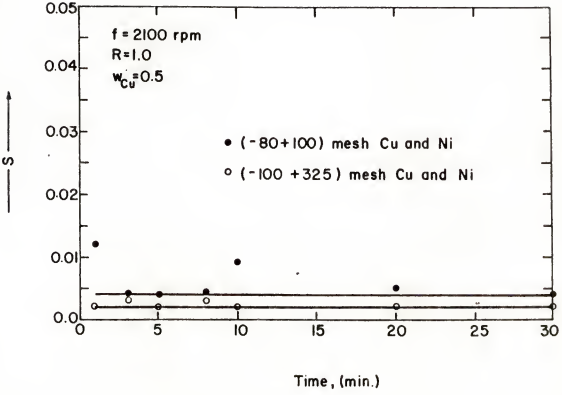

Figure 29. The influence of size distribution on the rate of blending for a binary mixture having a radius ratio of 1.0.

during blending thus reducing the probability for a particle to migrate. The results are shown in Figures 30 and 31.

In Figure 30 both compositions are independent of time in contrast to Figure 28 in which there was a time dependence for the first 5 minutes at $w_f = 0.1$. The reduction of the time dependent portion is attributed to a more efficient transport of powder to the turbulent zone with less percolation in the initial stages. For the time independent portions of the curve, there is no change as a result of the wider distribution. In Figure 31 there is a significant increase in the level of homogeneity as a result of the wider distribution. This is because of the alteration of the interparticle geometry which reduces the percolation process. The reason there was no reduction in s for $w_f = 0.1$ is that the size distribution did not cause a sufficient alteration of the interparticle geometry to effect the percolation process.

Discussion and Summary

It has been demonstrated that blending under vibratory conditions is dependent on the interrelationship between the turbulent zone for diffusive blending and the convective zones for mass transport. This is significant in that the benefits of the mechanisms of blending are realized while their detriments are diminished. Thus the diffusive zone acts to quickly disperse particle clusters which are

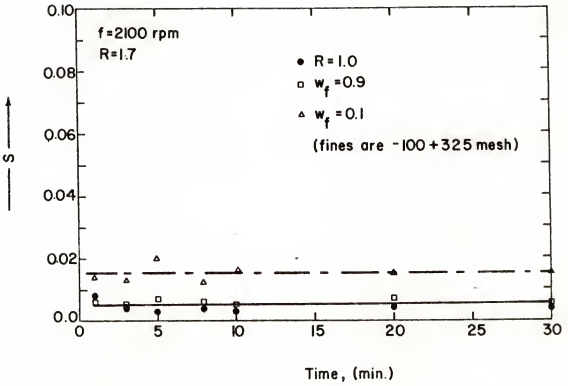

Figure 30. The influence of size distribution on the rate of blending for a binary mixture having a radius ratio of 1.7 (w_f = 0.1 and 0.9).

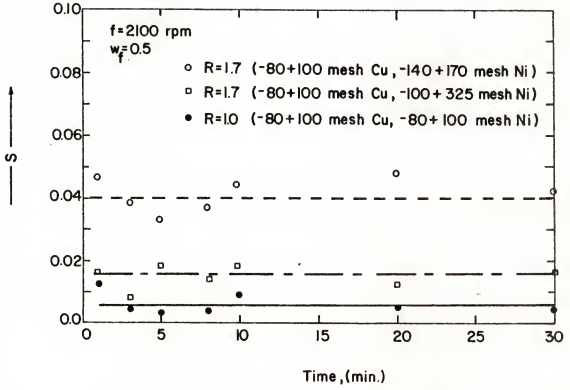

Figure 31. The influence of size distribution on the rate of blending for a binary mixture having a radius ratio of 1.7 (w_f = 0.5).

the detriments of convective blending and the convective zones, due to their stability, maintain the "random state" which was attained in the turbulent zone by diffusion. By the restriction of the size of the turbulent zone, size segregation which is characteristic of the turbulent zone is minimized.

In general, the vibratory blending process was observed to be mainly dependent on the interrelationship between the energetics of the process and the connectivity of the particle mass. Thus, in the upper layers of particles, motion was of a diffusive nature due to its low connectivity, whereas, deeper in the stack particle movement was by convection. It is the balance between these two zones which results in effective blending.

Also, of importance is the nature and interparticle geometry of the initial powder blend. For powder blends having the same average particle size it was shown that high degrees of homogeneity are attainable. Powder blends with wide size distributions may, in fact, actually enhance self-blending. For particle blends that have particle size differences it was demonstrated that the limit for the radius ratio, before percolation becomes dominant, is approximately 2.4. For a range of size ratios below 2.4, it was seen that the percolation process is relatively insensitive to size ratio. Furthermore, the percolation process can be reduced by alteration of the bed geometry

by either making the finer component the major phase or by changing the effective channel size by judicious use of the particle size distribution.

It was seen that by first analyzing the blending system on a fundamental scale, the true nature of the process was realized. That is, that vibratory blending is not appropriately classified by either the convective or the diffusive mechanism, but rather by a combination of the two.

CHAPTER VI
CONCLUSIONS

The objective of this study has been the development of a fundamental understanding of the role of compositional inhomogeneities at various stages of powder processing. For sintering and packing of binary mixtures that have large size ratios, mathematical procedures were derived to enable the recognition of the influence of compositional inhomogeneities. A model was presented to describe the fundamental interaction of particles during the blending process in order to understand the creation of inhomogeneities during vibratory blending. The results of these studies follow.

For the packing of binary powder mixtures, a procedure was developed for calculating the specific volume assuming the Furnas model is valid on a local scale. This assumption was shown to be valid for mixtures of glass microbeads which have a size ratio of 13:1 or greater. The procedure involves obtaining compositional inhomogeneity data for a body and constructing either a frequency or cumulative frequency curve. By integrating the curve, it is possible to calculate the specific volume of the body. This specific volume represents the Furnas specific

volume for an inhomogeneous mixture, and equals the bulk specific volume of the body if the Furnas model is valid. Assuming the Furnas model is valid, inequality of the specific volumes implies there is an additional factor leading to the deviation from the theoretical values. Therefore, the contributions to the specific volume from compositional variations can be mathematically eliminated. Thus, deviations from the theoretical predictions due to other powder characteristics that may be of importance to the process can be studied.

The above methodology has been applied to the sintering of inhomogeneous mixtures. From the developed mathematical base, a similar analysis can be used to recognize the effects of compositional inhomogeneities. This allows the study of the role of fine to coarse particle contacts in the creation of stresses and strain which can either enhance or retard the sintering process. Thus, the use of the developed methodologies could lead to a more fundamental understanding of the sintering and packing behavior of powders.

Fundamentally, the blending of powders was shown to depend on the interaction between the energetics of the process and the connectivity (i.e. stability) of the particle stack. In vibratory blending this relation gives rise to the turbulent zone for diffusive blending and the convective zones for mass transport. It has been demonstrated

that the combination of the two mechanisms of blending result in the reduction of processes that give rise to inhomogeneity.

APPENDIX

COMPUTER PROGRAMS (APL)

A. Calculation of the specific volume assuming a normal distribution.

```
     ∇ CURVE
[1]    'S'
[2]   START:S←□
[3]    YCB←0
[4]    NYCB←0
[5]    VVV←0
[6]   GO:→(YCB>1)/GOING
[7]    DISTR
[8]    CALC
[9]    VVV←VVV,VV
[10]   NYCB←NYCB,NYCB1
[11]   YCB←YCB+0.05
[12]   →GO
     ∇
```

B. Calculation of q_I, q_{II}, $(\tilde{w}_f)_I$ and $(\tilde{w}_f)_{II}$ from the normal distribution.

```
     ∇ DISTR
[1]    YC←0.01×⍳(⌊YCS×100)
[2]    Z←(YC-YCB)÷S
[3]    P←0.399××-0.5×Z*2
[4]    QC1←+/P×0.01÷S
[5]    YCB1←(+/P×YC×0.01)÷(+/P×0.01)
[6]    YC←YCS+0.01×⍳(100-(⌊YCS×100))
[7]    Z←(YC-YCB)÷S
[8]    P←0.399××-0.5×Z*2
[9]    QC2←+/P×0.01÷S
[10]   YCB2←(+/P×YC×0.01)÷(+/P×0.01)
[11]   AAA←QC1+QC2
[12]   QC1←QC1÷AAA
[13]   QC2←QC2÷AAA
[14]   YC←0.01×⍳100
[15]   Z←(YC-YCB)÷S
[16]   P←0.399××-0.5×Z*2
[17]   NYCB1←(+/P×YC)÷(+/P)
[18]   NYFB1←1-((+/P×YC)÷(+/P))
     ∇
```

C. Calculation of the local Furnas specific volume.

```
    ∇ CALC
[1]   VBB2←VCC×YCB2
[2]   VBB1←VFF-(VFP-VOO)×YCB1
[3]   VV←(QC1×VBB1)+(QC2×VBB2)
    ∇
```

D. Calculation of the specific volume assuming the Lacey distribution for a series of average compositions.

```
    ∇ FINAL
[1]   BASEDATA
[2]   'T'
[3]   T←⍬
[4]   SQ←0
[5]   WFB←0
[6]   V6←0
[7]  TO:LACEY
[8]   V6←V6,VVCC
[9]   DQ←DQ1,DQ2
[10]  SQ1←(+/(((WF-WFB)*2)×DQ))*0.5
[11]  SQ←SQ,SQ1
[12]  WFB←WFB+0.1
[13]  →(WFB>1)/STOP
[14]  'ONE'
[15]  →TO
[16] STOP:V←1↓V
[17]  WFB←0,0.1×⍳10
[18]  V6←1↓V6
[19]  SQ←1↓SQ
    ∇
```

E. Calculation of w_f^* (YFS).

```
    ∇ BASEDATA
[1]   VO←1
[2]   VF←2
[3]   VC←2
[4]   YFS←(VC-VO)÷(VF+VC-VO)
[5]   YCS←1-YFS
[6]   YFM←(VC-VO)÷VC
[7]   YCS←(⌊((YCS×100)+0.5))÷100
    ∇
```

F. Calculation of the specific volume from the Lacey distribution assuming a single average composition.

```
     ∇ LACEY
[1]    CON
[2]    WFS←YFS
[3]    WF1←(WF≤WFS)/WF
[4]    WF2←(WF>WFS)/WF
[5]    V1←VC×(1-WF1)
[6]    V2←VO+(VF-VO)×WF2
[7]    V←V1,V2
[8]    R←⍒V
[9]    AA←+/R
[10]   SSS←0
[11]   M←1
[12] VALVE:RR←R[⍳M]
[13]   SS←+/RR
[14]   M←M+1
[15]   SSS←SSS,SS
[16]   →(M>101)/PETE
[17]   →VALVE
[18] PETE:Q←SSS[1+⍳101]÷AA
[19]   PP←⌊(WF1)
[20]   →(PP=0)/LINE
[21]   →(PP=101)/LINE4
[22] LINE2:Q1←Q[PP]
[23] LINE3:Q2←1-Q1
[24]   QQQ1←Q[⍳PP]
[25]   QQ1←0,QQQ1
[26]   QQ11←¯1↓QQ1
[27]   DQ1←QQQ1-QQ11
[28]   WFSQ1←(÷Q1)×(+/WF1×DQ1)
[29]   QQQ2←(Q≥Q1)/Q
[30]   QQ2←1↓QQQ2
[31]   QQ22←¯1↓QQQ2
[32]   DQ2←QQ2-QQ22
[33]   WFSQ2←(÷Q2)×(+/WF2×DQ2)
[34]   →OK
[35] LINE:WFSQ1←0
[36]   Q1←0
[37]   Q2←1
[38]   WFSQ2←WFB
[39]   →OK
[40] LINE4:WFSQ2←0
[41]   Q1←1
[42]   Q2←0
[43]   WFSQ1←WFB
[44] OK:VB1←VC×(1-WFSQ1)
[45]   VB2←VO+(VF-VO)×WFSQ2
[46]   VVCC←(Q1×VB1)+Q2×VB2
     ∇
```

G. Calculation of the Lacey distribution.

```
     ∇ CON
[1]    N←1
[2]    WWF←0
[3]    Q←⍳20
[4]    XX←0,0.01×⍳100
[5]  FIRST:X←XX[N]
[6]    A←*-((Q*2)×(01*2)×T)
[7]    B←10(Q×WFB×01)
[8]    D←20(Q×X×01)
[9]    C←(2÷01)×A×B×D÷Q
[10]   CC←+/C
[11]   WF←WFB+CC
[12]   WWF←WWF,WF
[13]   N←N+1
[14]   →(N>101)/SECOND
[15]   →FIRST
[16] SECOND:NN←1+(⍳101)
[17]   WF←⌽WWF[NN]
     ∇
```

H. Calculation of the specific volume assuming fines sinter only and inhomogeneity follows a normal distribution.

```
     ∇ SINTER
[1]    VOO←1
[2]    VCC←2
[3]    VFF←1
[4]  START:S←⍞
[5]  HERE:→(VFF>2)/THERE
[6]    YCS←0
[7]    YCS←VFF÷(VFF+VCC-VOO)
[8]    VFF,YCS
[9]    YCB←0
[10]   NYCB←0
[11]   VVV←0
[12] GO:→(YCB>1)/GOING
[13]   DISTR
[14]   CALC
[15]   VVV←VVV,VV
[16]   NYCB←NYCB,NYCB1
[17]   YCB←YCB+0.05
[18]   →GO
[19] GOING: 14 3 DFT NYCB AND VVV
[20]   VFF←VFF+0.2
[21]   →HERE
[22] THERE:'END'
     ∇
```

I. Calculation q_I, q_{II}, q_{III}, $(\tilde{w}_f)_I$, $(\tilde{w}_f)_{II}$ and $(\tilde{w}_f)_{III}$ from the normal distribution (see Equation (31)).

```
     ∇ DISTRQ
[1]    YC←0.01×⍳(⌊YCM×100)
[2]    Z←(YC-YCB)÷S
[3]    P←0.399××-0.5×Z*2
[4]    QC1←+/P×0.01÷S
[5]    YCB1←(+/P×YC×0.01)÷(+/P×0.01)
[6]    YC←YCM+0.01×⍳(⌊G×100)
[7]    Z←(YC-YCB)÷S
[8]    P←0.399××-0.5×Z*2
[9]    QC3←+/P×0.01÷S
[10]   YCB3←(+/P×YC×0.01)÷(+/P×0.01)
[11]   YC←YCS+0.01×⍳(⌊YCS×100)×0.01)×100)
[12]   Z←(YC-YCB)÷S
[13]   P←0.399××-0.5×Z*2
[14]   QC2←+/P×0.01÷S
[15]   YCB2←(+/P×YC×0.01)÷(+/P×0.01)
[16]   AAA←QC1+QC2+QC3
[17]   QC1←QC1÷AAA
[18]   QC2←QC2÷AAA
[19]   QC3←QC3÷AAA
[20]   YC←0.01×⍳100
[21]   Z←(YC-YCB)÷S
[22]   P←0.399××-0.5×Z*2
[23]   NYCB1←(+/P×YC)÷(+/P)
[24]   NYFB1←1-NYCB1
[25]   →(NYFB1≥0.333)/HOG2
[26]   VI←(2×NYCB1)
[27]   →HOG3
[28] HOG2:VI←⍳1+NYFB1)
[29] HOG3:
     ∇
```

J. Calculation of the specific volume assuming fines and coarse sinter and inhomogeneity follows a normal distribution.

```
     ∇ SINTERALL
[1]    S←⍬
[2]    VOO←1
[3]   START:VCC←⍬
[4]    VFF←⍬
[5]    WFM←0
[6]    YCS←0.67
[7]    YFS←1-YCS
[8]    WFM←÷(1+VFF)
[9]    YCM←1-WFM
[10]   G←YCS-YCM
[11]   VMM←2×(1-WFM)
[12]   VFS←VCC×(1-YFS)
[13]   VFF,VCC,WFM
[14]   YCB←0
[15]   DELV←0
[16]   NYCB←0
[17]   NYFB←0
[18]   VVV←0
[19] HERE:→(VFF=1)/THERE
[20] THERE:→(VCC=1)/OUT
[21] GO:→(YCB>1)/GOING
[22]   DISTRQ
[23]   YFB3←1-YCB3
[24]   K←VFS-VMM
[25]   KK←WFM-YFB3
[26]   KKK←WFM-YFS
[27]   VBB3←VMM+K×(KK÷KKK)
[28]   VBB2←VCC×YCB2
[29]   VBB1←VFF-(VFF-VOO)×YCB1
[30]   VV←(QC1×VBB1)+(QC2×VBB2)+(QC3×VBB3)
[31]   DEL←(VI-VV)÷VI
[32]   VVV←VVV,VV
[33]   DELV←DELV,DEL
[34]   NYFB←NYFB,NYFB1
[35]   YCB←YCB+0.05
[36]   →GO
[37] GOING: 10 3 DFT NYFB AND VVV AND DELV
[38]    →START
[39] OUT:'END'
     ∇
```

BIBLIOGRAPHY

[1] C. C. Furnas, "The Relations Between Specific Volume, Voids and Size Composition in Systems of Broken Solids of Mixed Sizes," Department of Commerce - Bureau of Mines, R.I. 2894, October 1928.

[2] A. E. R. Westman and H. R. Hugill, "The Packing of Particles," J. Am. Ceram. Soc., 13[10] 767-69 (1930).

[3] R. K. McGeary, "Mechanical Packing of Spherical Particles," ibid, 44[10] 513-22 (1961).

[4] F. N. Rhines, "Dynamics of Particle Stacking," in THE SCIENCE OF CERAMIC PROCESSING BEFORE FIRING, G. Y. Onoda, Jr. and L. L. Hench, eds., J. Wiley Interscience, New York, 321-41 (1978).

[5] M. J. O'Hara and I. B. Cutler, "Sintering Kinetics of Binary Mixtures of Alumina Powders," Proceedings of the British Ceramic Society; Fabrication Science 2, No. 12 145-54, (1969).

[6] R. L. Coble, "Effects of Particle-Size Distribution in Initial-Stage Sintering, J. Am. Ceram. Soc., 56[9] 461-66 (1973).

[7] G. Y. Onoda, Jr., "Green Body Characteristics and Their Relationship to Finished Microstructure," in CERAMIC MICROSTRUCTURES--'76, R. M. Fulrath and J. Pask, eds., Westview Press, Boulder, Colo., 163-81 (1976).

[8] J. C. Williams, "The Mixing of Dry Powders," Powder Tech., 2, 13-20 (1968/9).

[9] N. Harnby, "A Comparison of the Performance of Industrial Solids Mixers Using Segregating Materials," Powder Tech., 1, 94-102 (1967).

[10] P. M. C. Lacey, "Developments in the Theory of Particle Mixing," J. Applied Chemistry (London) 4, 257-68 (1954).

[11] H. E. Rose and D. J. Robinson, "The Density of Packing of Two-Component Mixtures," Powder Met., 8[15] 20-38 (1965).

[12] D. W. Fuerstenau and J. Fouladi, "Degree of Mixedness and Bulk Density of Packed Particles," Bull. Am. Ceram. Soc., 46[9] 821-23 (1967).

[13] H. M. Walker and J. Lev, in ELEMENTARY STATISTICAL METHODS, 101, Holt, New York, (1958).

[14] R. Hogg, D. Cahn, T. Healy and D. W. Fuerstenau, "Diffsional Mixing in an Ideal System," Chemical Engineering Science, 21, 1025-38 (1966).

[15] S. S. Weidenbaum and C. F. Bonilla, "A Fundamental Study of the Mixing of Particulate Solids," Chemical Engineering Progress, 51, 27-36J (1955).

[16] R. Blumberg and J. S. Maritz, "Mixing of Solid Particles," Chemical Engineering Science, 2, 240-46 (1953).

[17] ASTM Designation: B243-70, Annual Book of ASTM Standards, Part 7, 235-39 (1970).

[18] R. Hogg, "Mixing and Segregation in Particulate Materials," Earth and Mineral Sciences, 40[6] 41-44 (1971).

[19] M. B. Donald and B. Roseman, "Industrial Aspects of Mixing and De-Mixing," Brit. Chem. Eng., 7[12] 922-23 (1962).

[20] H. Campbell and W. C. Bauer, "Cause and Cure of Demixing in Solid-Solid Mixers," Chem. Eng., 73[18] 179-85 (1966).

[21] M. L. Roessler and H. C. Willis, "Mixing with Vibrations," Bull. Am. Ceram. Soc., 48[3] 284-86 (1969).

[22] M. D. Ashton and F. H. H. Valentin, "The Mixing of Powders and Particles in Industrial Mixers," Trans. Inst. Chem. Engrs., 44, T166-88 (1966).

[23] J. C. Williams and M. I. Khan, "The Mixing and Segregation of Particulate Solids of Different Particle Size," Chem. Eng., London, 269, 19-25 (1973).

BIOGRAPHICAL SKETCH

Gary Lynn Messing was born April 13, 1951, in San Diego, California. Elementary education was obtained in Prattsburg, New York. His high school education was obtained at Canisteo, New York, Ilwaco, Washington, and Hornell, New York, culminating in graduation in June, 1969. He entered the New York State College of Ceramics at Alfred University in Alfred, New York, in 1969 and graduated with a Bachelor of Science in Ceramic Engineering in 1973. While attending Alfred University, he spent one semester at Friedrich-Alexander University in Erlangen, West Germany, in 1972. Since graduation he has been a graduate research assistant in the Department of Materials Science and Engineering at the University of Florida in Gainesville and received a Master of Engineering degree in 1975. He has since been pursuing a Doctor of Philosophy degree in the same department.

He has published papers in the area of research outlined in this dissertation. He is a member of Blue Key, Keramos, and Alpha Sigma Mu honoraries and has been cited in Who's Who in American Universities and Colleges. His professional memberships include the American Ceramic

Society, Society of Mining Engineers of AIME and the National Institute of Ceramic Engineers.

I certify that I have read this study and that in my opinion it conforms to acceptable standards of scholarly presentation and is fully adequate, in scope and quality, as a dissertation for the degree of Doctor of Philosophy.

George Y. Onoda, Jr., Chairman
Associate Professor of Materials Science and Engineering

I certify that I have read this study and that in my opinion it conforms to acceptable standards of scholarly presentation and is fully adequate, in scope and quality, as a dissertation for the degree of Doctor of Philosophy.

Frederick N. Rhines
Professor of Materials Science and Engineering

I certify that I have read this study and that in my opinion it conforms to acceptable standards of scholarly presentation and is fully adequate, in scope and quality, as a dissertation for the degree of Doctor of Philosophy.

Robert T. DeHoff
Professor of Materials Science and Engineering

I certify that I have read this study and that in my opinion it conforms to acceptable standards of scholarly presentation and is fully adequate, in scope and quality, as a dissertation for the degree of Doctor of Philosophy.

Larry L. Hench
Professor of Materials Science and Engineering

I certify that I have read this study and that in my opinion it conforms to acceptable standards of scholarly presentation and is fully adequate, in scope and quality, as a dissertation for the degree of Doctor of Philosophy.

Richard L. Schaeffer
Professor of Statistics

This dissertation was submitted to the Graduate Faculty of the College of Engineering and to the Graduate Council, and was accepted as partial fulfillment of the requirements for the degree of Doctor of Philosophy.

December 1977

Dean, College of Engineering

Dean, Graduate School